Bioluminescence Imaging Applications in Cancer: A Comprehensive Review

Nour Alsawaftah, Afifa Farooq, Salam Dhou, *Member, IEEE*, and Amin F. Majdalawieh

***Abstract*—Bioluminescence imaging (BLI), an optical preclinical imaging modality, is an invaluable imaging modality due to its low-cost, high throughput, fast acquisition times, and functional imaging capabilities. BLI is being extensively used in the field of cancer imaging, especially with the recent developments in genetic-engineering, stem cell, and gene therapy treatments. The purpose of this paper is to provide a comprehensive review of the principles, developments, and current status of BLI in cancer research. This paper covers the fundamental BLI concepts including BLI reporters and enzyme-substrate systems, data acquisition, and image characteristics. It reviews the studies discussing the use of BLI in cancer research such as imaging tumor-characteristic phenomena including tumorigenesis, metastasis, cancer metabolism, apoptosis, hypoxia, and angiogenesis, and response to cancer therapy treatments including chemotherapy, radiotherapy, immunotherapy, gene therapy, and stem cell therapy. The key advantages and disadvantages of BLI compared to other common imaging modalities are also discussed.**

***Index Terms*—Bioluminescence Imaging, Molecular Imaging, Luciferase, Cancer Applications**

I. Introduction

CANCER is a complex multigenic disorder whereby cells divide uncontrollably, forming tumors. These tumors can invade neighboring tissues and spread to distal body locations in a phenomenon referred to as metastasis [1]. Cancer is one of the four major non-communicable diseases that are considered to be the leading causes of death worldwide [1]. According to the International Agency for Research on Cancer in 2018, around 18.1 million new cases of cancer were expected to be diagnosed and the death toll was expected to reach approximately 9.6 million deaths [1]. The most common ways of treating cancer include: (1) surgery, (2) chemotherapy, (3) radiotherapy, (4) targeted therapy, and (5) immunotherapy [2], [3]. It is difficult to predict the success of cancer therapy due to the uncertainties caused by the inherent complexity and heterogeneity of different types of cancer as well as the variability of the same type of cancer among patients. Therefore, monitoring the response of cancer to the administered treatment is essential in the treatment process. Imaging modalities such as positron emission tomography (PET), magnetic resonance imaging (MRI), computed tomography (CT), and ultrasound (US) are used to monitor the therapeutic response of various cancer types to a given therapy. Given the dynamic nature and adaptability of tumors, the employed diagnostic imaging modality for treatment response monitoring must be able to "keep up" with the continuous evolution of tumors. Thus, real-time dynamic imaging during cancer treatment sessions is needed to enable the unveiling of the evasive response patterns of tumors and make it possible to devise better and more personalized treatment plans [2], [4]. In this respect, molecular imaging is emerging as an attractive route for monitoring therapeutic responses.

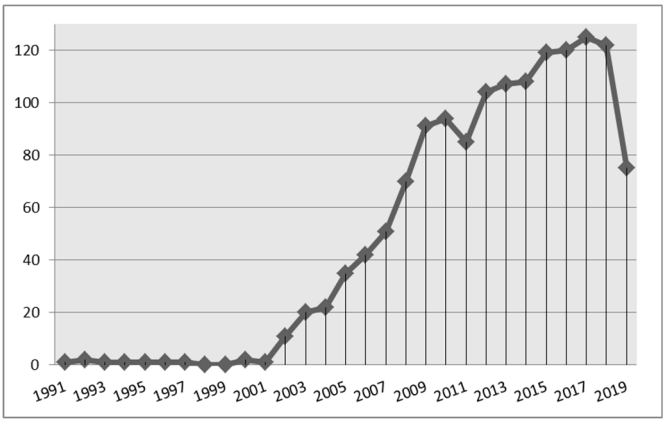

Fig. 1. Number of studies on applications of BLI in cancer (data obtained from Web of Science database up to October 2019).

Molecular imaging is a noninvasive imaging technique that allows the visualization of fundamental biomolecular and cellular processes through the detection of signals originating from the interaction of injected radiolabeled tracers with a specific cellular target or by measuring optical signals emitted by enzyme-substrate reactions *in vivo* [1]. Studying molecular

This paragraph of the first footnote will contain the date on which you submitted your paper for review. It will also contain support information, including sponsor and financial support acknowledgment. For example, "This work was supported in part by the U.S. Department of Commerce under Grant BS123456."

N. Alsawaftah is with the Biomedical Engineering Graduate Program, American University of Sharjah, Sharjah, UAE, (e-mail: g00051790@alumni.aus.edu).

A. Farooq is with the Biomedical Engineering Graduate Program, American University of Sharjah, Sharjah, UAE, (e-mail: g00051241@alumni.aus.edu).

S. Dhou is with the Department of Computer Science and Engineering and the Biomedical Engineering Graduate Program, American University of Sharjah, Sharjah, UAE (e-mail: sdhou@aus.edu).

A. F. Majdalawieh, is with the Department of Biology, Chemistry, and Environmental Sciences and the Biomedical Engineering Graduate Program, American University of Sharjah, Sharjah, UAE (e-mail: amajdalawieh@aus.edu).

and cellular changes is of great importance because alterations on this level usually precede palpable anatomical and physiological changes associated with disease emergence and/or progression. Therefore, the early identification of such differences can lead to improved and better optimized therapies particularly in the field of cancer [5]. Cancer molecular imaging permits the *in vivo* characterization and measurement of molecular and cellular events that have the potential to enhance cancer diagnosis and staging especially tumor detection and characterization at an earlier treatable stage without the need for invasive procedures [6], [7]. A number of molecular imaging methods exist, including those based on nuclear imaging technologies such as PET, and single photon emission tomography (SPECT) and optical molecular imaging. Optical molecular imaging is an imaging technique that measures light from either endogenous sources or exogenously administered fluorochromes that bear information about biological processes on a microscopic scale [8]. Optical molecular imaging is divided into fluorescence imaging (FLI) and bioluminescence imaging (BLI). However, the main area of focus in this paper is BLI. A trend showing increasing interest in the field of BLI is depicted in Fig. 1.

II. Bioluminescence Imaging (BLI)

A. Overview

Bioluminescence, the ability of organisms to produce light, has been observed widely in fireflies, fungi, beetles, bacteria and marine creatures. This light is generally produced by a two-step oxidative mechanism: (1) two molecules/proteins are combined in the presence of oxygen to form an energy-rich molecule; (2) this energy-rich molecule gives off a photon of light to return to its stable state [8]. The applications of bioluminescence in imaging have attracted the attention of researchers since the mechanisms behind bioluminescence have been discovered. BLI uses the natural process of converting chemical energy into light, or photons, by using enzymes known as luciferases or photoproteins and combining them to luciferins, the substrates. These substrates are oxidized by the enzymes, where some of which may require cofactors such as ATP, Mg^{2+}, Ca^{2+}, etc., and thus emit light at different wavelengths [8], [9]. Hastings conducted a review in which he deduced that these wavelengths were dependent on four factors: (1) luciferases/photoproteins, (2) luciferins, (3) optical biological filters, and (4) accessory luminophores [10]. The wavelength/color of visible light emitted has major implications for *in vivo* BLI [10]. For example, the depth of overlying tissue over the region of interest plays a major role in which organisms can be imaged using BLI. As seen in Fig. 2, common luciferase reporters exhibit a 10-fold decrease in imaging sensitivity per centimeter of depth [11]. Therefore, BLI is only suitable for imaging small animals such as mice. However, BLI is a pivotal imaging modality in preclinical research due to the fact that animals currently used in research have no intrinsic bioluminescence, which means that the background signal from these animals is next to none. Therefore, this modality surpasses all others in terms of sensitivity [11]. Due to emission improvement, a recent development in BLI has led to the visualization of a single tumor cell from a factor of 100 to 1000 compared to conventional techniques [12].

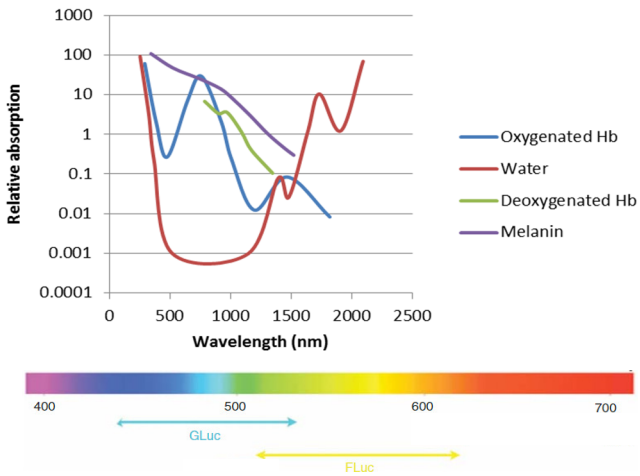

Fig. 2. Absorption spectra depicting the importance of red-shifted BLI reporters; the optical window demonstrates the area where there is the least absorbance by major optical absorbers (e.g. melanin, hemoglobin, oxyhemoglobin and water). Common optical reporters for BLI have also been shown: GLuc, *Gaussia (Gaussia princeps)* luciferase; FLuc, Firefly (*Photinus pyralis*) luciferase.

Since BLI has a wide range of applications in preclinical imaging, especially in cancer research, as well as having high sensitivity and fast imaging times, it is the modality of choice for *in vivo* tumor biology studies in animals. As luciferases are not endogenously expressed in most animals, BLI is carried out using either transgenic animals, with animal DNA modified with the specific luciferase reporter gene to obtain luciferase expression *in vivo*, or by xenograft insertion of the transfected or virally transduced cancer cells into the animal body. In the latter, there is an extremely high sensitivity due to the lack of background signals from bioluminescence. This makes the BLI signal more sensitive as genes for luciferases/photoproteins are duplicated upon cell division and gene expression of the modified DNA. The xenografted animals are injected with a luciferin substrate, allowing the tumor cells to bioluminesce. Since the substrate-enzyme reactions require co-factors such as ATP and oxygen, the high metabolic activity of cancer cells means that the tumor microenvironment would appear more bioluminescent than the surrounding tissue [13]–[15]. After substrate injection, the animals can be imaged using highly sensitive light detectors immediately or within minutes due to the fast biodistribution of the substrates, as the bioluminescent signals of firefly luciferases plateau approximately 10 minutes after intraperitoneal injection [16]. The light detectors used in this imaging modality are called charge-coupled device (CCD) cameras and are commercially available. They obtain a digitized and quantifiable 2D map of light intensity within the field-of-view (FOV). These images are then overlaid on a photograph of the test subjects taken under normal light conditions. For this reason, the animals are anesthetized prior to imaging to ensure no movement [11], [14]. Several BLI studies were conducted using different reporter systems that resulted in luciferase-luciferin reactions emitting light with different spectra and tissue penetration depths (Fig. 3) [14]. Therefore, the purpose of this paper is twofold: first, to give the reader a background of BLI systems along with their main

advantages and disadvantages; second, to expand the reader's understanding of the major applications of BLI within the field of cancer research namely imaging of tumor-related phenomena including tumorigenesis, metastasis, angiogenesis, tumor hypoxia, apoptosis, cancer metabolism, as well as imaging of response to cancer treatments including chemotherapy, radiotherapy, gene therapy, and stem cell therapy.

B. BLI reporter genes, reporters and substrates

1) Gene reporters and their use in imaging and therapy

There are two ways to express luciferases *in vivo*: either by transfecting bacteria with reporter genes or transfecting cancer cells or animal embryos with luciferase reporters (refer to Fig. 4 for general technique). The term "gene expression" in this paper refers to the transcription of a gene followed by the translation of the resulting mRNA leading to protein synthesis. Promoters and other regulatory sequences control the amount of mRNA produced, which in turn controls the amount of protein produced. Promoter activity can be determined by measuring the transcribed signal of the gene being controlled by that promoter, whereas protein levels can be assessed by detection of the fusion proteins [17]. Based on this notion, dual-reporting system assays reporting two different transcriptional events and multi-color assays with different reporting systems have been developed [18]. Noguchi and Golden summarized the routes for one time-point gene quantification, temporal gene quantification, spatiotemporal gene quantification, temporal protein quantification, and spatiotemporal protein quantification in the field of BLI [17]. Signal transduction, receptor activation, transcription factor activity, and post-transcriptional (e.g. RNA processing, RNA splicing, and RNA interference) can be exploited to assess cancer progression and cancer therapy efficacy [13].

2) Luciferase/photoprotein-luciferin reporter systems

Bioluminescence reporters can be subdivided into two main types: luciferases and photoproteins. Luciferases catalyze luciferins to oxyluciferins, the light emitted from the luciferin-luciferase reaction depends on the resultant oxyluciferin formed, whereas the light from the luciferin-photoprotein reaction depends on the concentration of photoproteins. The latter reaction is mainly used to report the concentrations of Ca^{2+}, Mg^{2+}, ATP, H_2O_2, or superoxides [19], [20]. These BLI reporters can be further classified into bacterial, fungal, small terrestrial invertebrates, marine organisms, and synthetic or bioengineered reporters (Table I) [21]–[23]. Of the non-synthetic luciferases, firefly was found to be the most sensitive for *in vivo* applications [19]. Xu and colleagues presented a brief summary of beetle, bacterial, and marine luciferases used for BLI *in vivo* applications [24]. In contrast to luciferins, luciferases or photoproteins are unique to their corresponding species, and thus, only a few have been characterized and modified for research purposes. The three most common reporters are firefly luciferase (FLuc), Renilla luciferase (RLuc), and Gaussia luciferase (GLuc). Their reaction mechanisms and co-factor requirements are shown in Fig. 3.

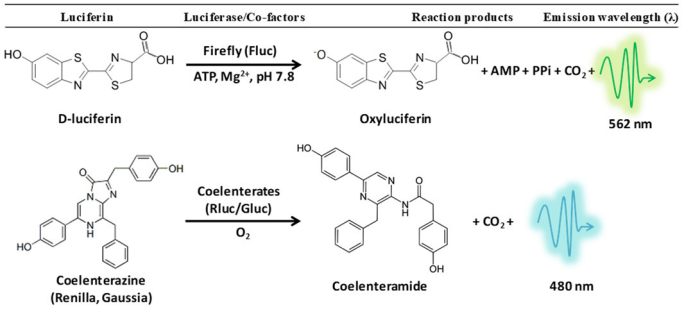

Fig. 3. Luciferase-luciferin reactions for the three most commonly used reporter systems (FLuc, GLuc, and RLuc). Emission wavelengths are also specified. Note that FLuc emits green light, close to the NIR window, and thus, is more ideal for *in vivo* imaging due to increased penetration depths.

The use of red-shifted reporter systems, which are close to the near-infrared (NIR) regions, is crucial for *in vivo* applications due to the high penetration depth. Table I presents several reporters that have been used in studies cited in this paper and

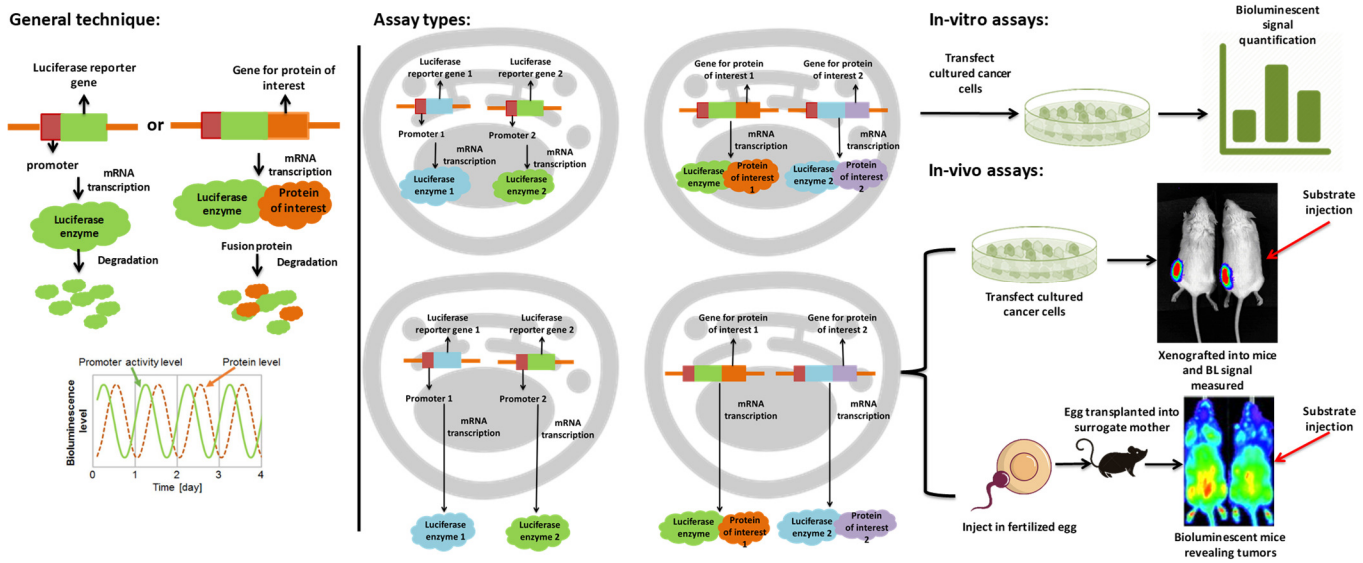

Fig. 4. Gene reporting used in BLI (encoding areas may vary depending on application); several bioluminescence assays have been developed (the second reporter gene can be either function as a control reporter gene or a different luciferase reporter gene). Information is summarized from studies cited in this paper. Note: This is a generalized version for BLI.

TABLE I
CLASSIFICATION AND THE TYPES OF REPORTER SYSTEMS ALONG WITH THEIR ROLE IN IMAGING FOR CANCER APPLICATIONS

Enzyme	Luciferin	Application in imaging cancer	Co-factors	Comments	Relevant References
Terrestrial					
Beetle Luciferases					
Photinus pyralis (from fireflies, FLuc) and variants (Luc2)	D-luciferin	Tumor metabolism, burden, and angiogenesis; tumor evaluation after therapy	ATP, Oxygen	Has numerous variants and is the most cited in studies with its most useful applicability being *in vivo* analysis due to its red-shifted emission spectra; quantum yield: 41%	[19], [24], [52], [150], [151]
Synthetic/Engineered systems					
AkaLumine	AkaLumine	Single cell monitoring for real-time imaging (new development in BLI)	ATP, Oxygen	100 – 1000 fold more sensitive than conventional systems	[12], [25], [26]
Split Luciferases					
BAR (AKT reporter using FLuc)	D-luciferin	Tumor growth; response to chemotherapy	ATP, Oxygen, Mg^{2+}	AKT measurements are an indication of resistance to cancer therapy as well	[69], [92], [152]
Caged Luciferases					
Photinus pyralis (from fireflies, FLuc)	Peroxy Caged Luciferin-1 (PCL-1)	Tumor metabolism	ATP, Oxygen, Mg^{2+}	Reaction of aryl boronic acid from PCL-1 with H_2O_2 or peroxynitrite to release D-luciferin	[89], [91], [153]
Bacterial					
Photorhabdus luminescens (modified for gram + or – bacteria)	$FMNH_2$	Imaging response to gene therapy	Long chain fatty aldehydes, Oxygen	Generally the luxABECD operon is introduced in E.coli due to their specificity to colonize tumor sites	[122], [154]–[156]
Marine					
Gaussia princeps (Gaussia luciferase, Gluc)	Coelenterazine	Tumor metastasis using stem cell imaging and therapy response	Oxygen	Reports 200 fold higher signal intensity compared to humanized Fluc and Rluc, suitable mainly for *in vitro* testing; broad emission spectrum extending to 600 nm	[19], [157], [158]
Renilla reniformis (RLuc) and variants (RLuc8 and RLuc8.6-535)	Coelenterazine	Multiplexed for imaging of therapy response to gene therapy	Oxygen	Quantum yield: 6%, therefore, cannot be used alone in *in vivo* applications	[19], [24]
Photoproteins					
Aequorin (derived from hydrozoan *Aequorea victoria*)	Coelenterazine	Tumor burden and response to therapy	Ca^{2+}, Oxygen	High Ca^{2+} specificity with 2 to 3 Ca^{2+} ions needed. Semilogarithmic light emission profile (could lead to misinterpretation of results if used alone)	[147], [159]
Synthetic/Engineered systems					
NanoLuc™ luciferase (NLuc) (derived from *Oplophorus gracilirostris*)	Furimazine (derived from coelenterazine)	Response to therapy(using genetic reporting)	Oxygen	NLuc found to be 79-fold brighter than FLuc on average and ~3 times smaller as well; high pH and thermal stability	[115], [160]–[162]
Bacterial					
Aliivibrio fischeri	$FMNH_2$	Tumor metabolism and hypoxia	Long chain fatty aldehydes, Oxygen	Mainly used for measurement of lactate concentrations	[163]–[166]

highlights the implications of each reporter on the image quality. Iwano and colleagues synthesized Akalumine-HCl salt, a luciferin, and demonstrated that it could saturate FLuc better than D-luciferin [25]. To further develop optimal enzymatic activity, they used the theory of natural reporter system evolution and performed directed evolution by using random gene mutations to create FLuc variants. Among the brightest variants, AkaLuc was yielded. The peak emissions were found to be 1000 times brighter (650 nm), leading to single cell imaging in freely moving animals [12], [25], [26].

In the case of the substrates or luciferins, research has found that they are conserved across species [20]. There are four main luciferins that have been discovered in and isolated from marine bioluminescent species: bacterial luciferin, a reduced riboflavin phosphate, dinoflagellate luciferin, vargulin or cypridina-type luciferin, and coelenterazine luciferin [20]. These luciferins are either ingested by the organism or produced *in vivo*, which means that, in terms of BLI, it has to be injected into the test subject. In general, substrate biodistribution is affected by: 1) the physiology of the animal; 2) the route of administration, either intraperitoneally or intravenously, 3) the flow of blood, 4) the capacity to bind to serum proteins, and 5) the level of inhibition due to anesthetics [27], [28]. Different types of reporter systems have been optimized for *in vivo* applications [24]:

- Synthetic/mutated luciferase: this system adds to/modifies the enzymes for improved function and increased light output.
- Synthetic luciferin analogs: luciferins are modified or tuned to exhibit application-specific properties or better biodistribution ability (i.e., more substrate accumulation at the site to be imaged to increase light output).
- Multiplexed systems: multiple luciferase-luciferin system tagging can be performed in the same subject, such as the expression of both FLuc and GLuc together, so that each system may monitor different biological processes. Different substrates ensure minimal cross talk and spectral un-mixing techniques can be used for identification of each system on images.

- Split luciferases: the luciferase enzyme is split apart into its C-terminus and N-terminus fragments with a protein or peptide inserted in the middle. Activation of the enzyme and the associated light output is only accomplished when the fragment in the middle interacts with the protein of interest.
- Caged luciferins: they are luciferins that cannot interact with their corresponding luciferases unless an enzymatic cleavage event occurs which can be used to target specific biological processes.
- Bioluminescence Resonance Energy Transfer (BRET) and Fluorescence by Unbound Excitation from Luminescence (FUEL): both systems incorporate FLI for imaging purposes. The emission of light from a BLI reporter system activates/excites that of the fluorescent chromophore. The main difference between BRET and FUEL is that in FUEL the emission and excitation chromophores have to be micrometers or centimeters away from each other, whereas, in BRET, they have to be nanometers away from each other. Usually, for BRET, both chromophores might be encoded within the same promoter sequence for close-chromophore expression.
- Bioluminescent enzyme-induced electron transfer (BioLeT): this system uses electron-donating moieties within luciferin analogs to act as an on/off switch for bioluminescence signals.

3) Instrumentation

Since detection of bioluminescence signals involves measuring light emission from the test subjects and due to the need for extreme sensitivity, the test subjects are enclosed in a dark box. Furthermore, due to the extensive and functional use of BLI in the field of medicine, PerkinElmer Inc. (Waltham, Massachusetts, United States) has commercialized their own 2D and 3D BLI systems, known as the IVIS spectrum imaging systems. The components of the IVIS system are depicted in Fig. 5. These systems integrate X-ray and CT technologies along with FLI to contribute to optical overlays for scans, providing a multimodal approach to BLI [29]. Most studies cited in this paper have used the IVIS *in vivo* imaging systems for bioluminescence measurements.

i.Main instruments of BLI system

- Luminometer: this is a sensitive photometer that can be used to detect bioluminescence signals from assays or tests on microplates or cuvettes. These use a sample chamber, sealed from ambient light, positioned as close to the detector as possible for maximum optical efficiency. It detects photon output using photomultiplier tubes (PMTs) or photodiodes. When an incident photon hits an electron, an amplification cascade is triggered. This cascade is noise-free, which makes it efficient for measurements. The PMTs are either present on the side of or the bottom of the sample chamber [30]. Commercialized luminometers are available from Promega Corp. (Madison, Wisconsin, USA), PerkinElmer Inc. (Waltham, Massachusetts, USA), and Titertek Berthold (Pforzheim, Germany). It is worthwhile to mention that the most sensitive luciferase reporter system found for *in vitro* testing is GLuc.

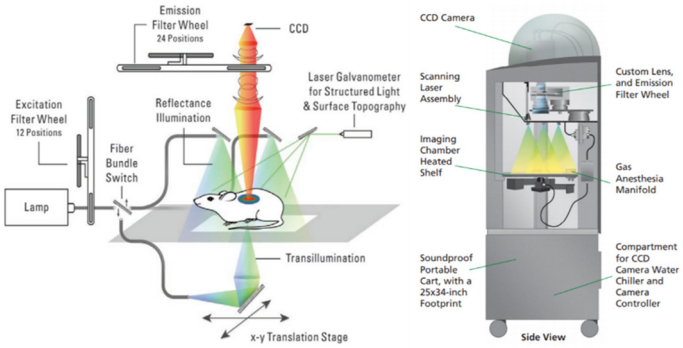

Fig. 5. Representation of imaging instrumentation (IVIS Spectrum system). Reproduced from [29].

However, the reader should note that it emits blue light (480 nm), and thus, it is not as sensitive for *in vivo* measurements [13].

- CCD camera: this camera is thermoelectrically cooled (-90ºC), to ensure low dark current and readout noise for capturing emitted light from test subjects. These cameras detect images in the blue to NIR wavelength range. In general, the CCD itself, is a non-color, back illuminated full frame image sensor that exhibits more than 85% quantum yields for light in the 400-750 nm range and 50% quantum yields for the 750-900 nm range. The photon measurements are digitized using a 16-bit A/D converter, and therefore, it has a dynamic range of 75,000 to measure high and very low signals with 2048 × 2048 pixels. It also has large aperture optics and is calibrated using a low-intensity, diffuse, flat field source that can be adjusted to a known radiance source, such as a phantom mouse. The camera converts the digital units into absolute physical units (Watts/square centimeters/steradian or photons/seconds/square centimeters/steradian) [29], [31]. This absolute unit can be used as a comparison unit between experiments and systems even when acquisition parameters are vastly different. Typically, relative counts or photons per second are only usable when acquisition parameters, relative animal position to camera, f-stop, region of interest, FOV dimensions, internal pixel binning, CCD temperature, background signal, and readout noise are exactly the same [31], [32]. The 2D image acquired has a pseudo-color scaling where red areas correspond to the highest amounts of light emission and blue or violet correspond to the lowest amounts of light emission [32].

Since 2D imaging provides only a relative measure of internal source brightness that limits the quantification of source depth and attenuation due to tissues, a need for 3D images arose. 3D systems for source localization and tissue-attenuation corrections have been developed. Wang and colleagues developed a system that would vertically rotate the stage while horizontally moving it to match the focal length of the camera [33]. In this system, two images are taken for the test subject: one in the dark for the bioluminescence signal and one with light for co-registration on the same pixel within the mouse volume. Several 3D imaging systems, measuring multispectral information (refer to Fig. 5 showing the IVIS Spectrum CT imaging system), have been developed with some

of them using multiple CCD cameras or mirrors for multi-view technology [31], [34]. CCD rotating camera systems, multiple CCD camera systems, and rotating stage systems have been used for 3D BLI imaging so far. Some have incorporated other modalities such as FLI and CT into the 3D BLI systems for biologically relevant and anatomically accurate localization (Fig. 6). A recent study applied the idea of low light transmittance, previously used in FLI, of fiber-optical bundles for high resolution imaging of BLI [35]. It also incorporated reflectance imaging to view structural details of organs and blood vessels. Since FLuc, the most commonly used luciferase reporter for *in vivo* imaging, has a broad emission spectrum ranging from 540-660 nm with peaks at 620 nm, multispectral imaging can be adequately used on it. This is done on the basis that blue-shifted light, towards the 540 nm side, will attenuate more *in vivo* while red-shifted light, towards the 660 nm side, will attenuate less with larger photon emissions detected at these wavelengths. In other words, bioluminescence signals from deeper sources will exhibit larger signals for images collected at the 660 nm wavelength than the ones collected at lower wavelengths. A series of scans with 20 nm increments are collected to measure source depth. This phenomenon is known as diffuse light imaging tomography (DLIT) and is widely used for BLI [36], [37].

ii.Other instrumentation

- CCD camera water chiller: this system cools the CCD device to sub-zero temperatures either cryogenically or thermoelectrically.
- Gas anesthesia manifold: this system generates oxygen containing 2% isoflurane (or other anesthetics depending on the system used) to anesthetize the mice and ensure no movement.
- Emission filter wheel or dichroic mirrors: the wheel is usually placed in front of the CCD camera to let light of only a single wavelength, adjusted according to the operator's needs, pass through to enable multispectral measurements. Dichroic mirrors perform the same function in addition to providing dual/multi view capabilities.
- Imaging chamber shelf/stage: this is where the test subjects are placed for imaging and it is usually heated to ensure maintenance of physiological body temperature.
- Imaging chamber: this chamber is completely dark and soundproof to ensure maximum sensitivity of measurements.
- Phantom mice/accessories: phantom mice may be provided by the vendor to calibrate the device. Other accessories include animal shield kits, animal isolation and chamber kits [29], [31], [36], [38].

Some considerations for improved bioluminescence signal sensitivity are: instrumentation, amount of hair, tissue depth between imaging instrument and region-of-interest (ROI), amount of substrate injected, and promoter activity levels leading to luciferase expression [32].

C. *Image acquisition, processing, and quality*

Many small animal imaging systems have been specifically designed for the detection of light-based technologies. Moreover, recent advances in instrumentation have resulted in

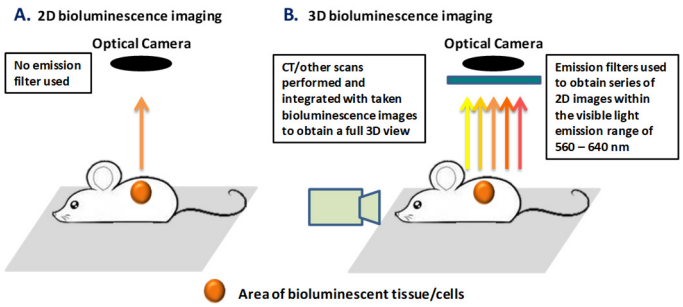

Fig. 6. A. 2D imaging system depicting greater light sensitivity due to acquiring full emission B. 3D acquisition using emission filters for different wavelengths.

systems with improved sensitivity and image quality [39]. CCD cameras are run by computers for image acquisition, processing and analysis [39]. At first, a digital image, which will serve as the reference for anatomic information, is taken during 0.2 seconds under very weak illumination. Next, the weak light is turned off and photon collection is started over various integration times. The total integration time depends on the expected amount of emitted light, however exposure times longer than 5 minutes usually do not further improve sensitivity. Software is then used to superimpose both images so that the location of the bioluminescent signal can be inferred with respect to the anatomical information acquired. Because BLI is a light-based imaging technology in which signal intensities are depth dependent, quantification of serial image acquisitions of the same animal can only be performed if the positioning and acquisition settings are identical over the time course of the experiment (Fig. 7) [5].

Current BLI systems can generate both 2D and 3D images. 3D images result from applied bioluminescence tomography (BLT). Traditionally, optical tomography involves sending visible or NIR light into the region or object of interest and reconstructs the distribution of internal optical properties such as absorption and scattering coefficients. Contrastingly, BLT depends on the reconstruction of an internal source of bioluminescence from BLI measurements at the object's surface [38], [40]–[42]. Mathematically, BLT is a source inversion problem based on boundary measurements, and hence, is a highly ill-posed inverse problem. The solution uniqueness for BLI can be improved through the incorporation of prior knowledge to regularize the problem, and by using an appropriate simplified model in turbid media [42], [43], [74]. The assumptions of this simplified model include [43]:

- Bioluminescence photon scattering predominates over absorption in tissue.
- Steady-state diffusion.
- Partial current boundary condition for a semi-infinite space.
- An initial order approximation to the photon energy fluence.
- Linear rate operator representing the fluence rate data for the internal source.

To estimate the position and intensity of a bioluminescence source, one can describe photon propagation through tissue by the diffusion approximation to Radiative Transfer Equation (RTE). RTE, also known as the linear Boltzmann equation, is

the most precise mathematical model used to describe photon propagation in biological tissues [41]–[43].

$$\frac{1}{c_n}\frac{\partial\varphi(r,t)}{\partial t} = -D\nabla^2\varphi(r,t) - \mu_a\varphi(r,t) + S(r,t) \quad (1)$$

where φ (r, t) is the isotropic fluency rate; D and μ_a are the diffusion and absorption coefficients, respectively; S(r,t) is the internal light source distribution and r(x, y, z) is the distance away from the source in time t. For steady-state diffusion, the photon fluence rate at the physical boundary can be expressed as a sum of contributions from the positive internal source $\varphi(r_s)$ and its negative image source above the tissue $\varphi(r_i)$, this is represented by Equation 2 and its expansion in Equation 3 [42], [43]:

$$\varphi(r) = \varphi(r_s) - \varphi(r_i) \quad (2)$$

$$\varphi(r) = S_0 e^{-\mu_{eff} r_s}\frac{(4\pi D)^{-1}}{r_a} - S_0 e^{-\mu_{eff} r_s}\frac{(4\pi D)^{-1}}{r_i} \quad (3)$$

Here $r_s = (z_s^2 + r^2)^{1/2}$ and $r_i = (z_i^2 + r^2)$ is the distance from the source and its image to point on the boundary, $\mu_{eff} = (\mu_a / D)^{1/2}$ is an effective attenuation coefficient, the surface radiance on the physical boundary is then given by [42], [43]:

$$L(r) = \frac{1}{4\pi}\varphi(r) + \frac{3}{4\pi}[\varphi(r_s)\Delta s + \varphi(r_i)\Delta_i] \quad (4)$$

$$\Delta_\alpha = \frac{z_\alpha}{r_\alpha^2}(1 + r_\alpha\mu_{eff})D, \text{for } \alpha = s, i \quad (5)$$

Mathematically, BLT is the source inversion problem to recover a known light source function from optical measurement on the domain boundary, utilizing detailed knowledge on the optical properties of biological medium under consideration. On one hand, the existence and uniqueness of solution to the BLT inversion problem has been extensively studied in literature, as RTE is highly dimensional and presents a serious challenge for its accurate numerical simulations [38]. On the other hand, the linearity of the BLT inversion problem makes it a regularization-free method unlike the FLI inversion problem that requires regularization-based methods [41]. With regards to acquisition time, images can be obtained within 1 second or they can take up to 10-20 minutes based on the signal intensity measured [16].

Improvements in imaging techniques and instrumentation have revolutionized early diagnosis and treatment of numerous pathologies. The accuracy of clinical diagnoses depends critically on the quality of images acquired using medical imaging modalities. In order to properly assess these images, a quantitative criteria is used. The spatial resolution of an imaging system is best defined as the smallest feature that can visualized or the smallest distance between two features such that these two features can be resolved individually and not appear as a single object [44]. BLI is characterized as having low spatial resolution (1-2 mm), which is due primarily to light quenching and scattering in biological tissues [19]. Moreover, the spatial resolution of BLI is strictly limited by the number of substrate molecules being catalyzed by the luciferase enzyme. However, this limitation is becoming less problematic with the emergence of multi-modal imaging and BLT capable of 3D image reconstruction and acquiring the signal at multiple angles [41], [45]. On the other hand, BLI signals tend to have high sensitivity and signal-to-noise ratio (SNR) This can be attributed to the fact that background luminescence is negligible compared to the signal produced by the luciferase catalytic reaction [41].

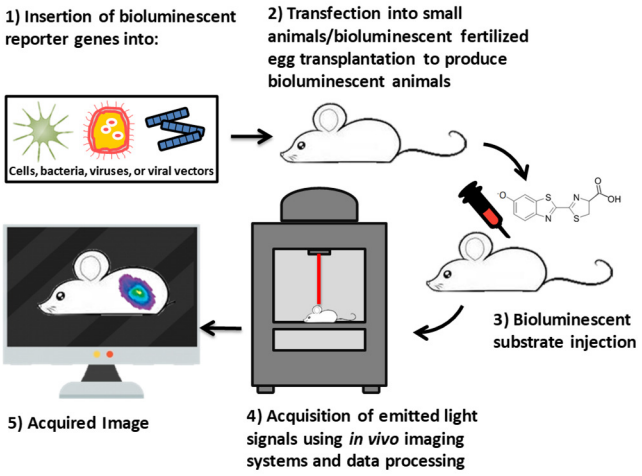

Fig. 7. Bioluminescence tomography system.

D. Limitations of BLI

BLI has numerous advantages including non-radioactivity, high sensitivity, relatively lower equipment costs, high throughput, short image acquisition times, relative ease of use, and minimal image post-processing requirements. Furthermore, BLI allows monitoring of tumor growth, metastasis, and response to treatment in preclinical cancer models without the need to euthanize the test animals [46]. A summary of the advantages and disadvantages of BLI, as compared to other common imaging modalities, is presented in Table II. FLuc bioluminescence activity is dependent on the presence of oxygen and ATP, and consequently, photons are only emitted from metabolically active cells. This facilitates the ready assessment of new therapeutic effects as light emission is proportional to the number of viable labeled cells [2]. The high sensitivity of BLI also allows for the early detection of tumors as malignant cells may be visualized using BLI at least 13 days before they form palpable tumors in certain xenograft models [46].

As with any other imaging modality, BLI has its advantages and its shortcomings. The main problems encountered when using BLI systems are discussed below:

- Signal quantification: it is difficult to standardize *in vitro* BLI assays because the relative light units (RLU) measured from the luciferase reactions are arbitrary units that vary from one photon detector to the other [41], [45]. Despite BLI not being an absolutely quantitative imaging approach, it allows tumor growth dynamics to be accurately determined by quantifying relative changes in light emission over time [46].
- Background control: even though BLI is characterized as having high sensitivity due to its low background noise, it is still recommended to include proper background controls such as using buffers or media that do not express the luciferase when conducting *in vitro* experiments [45].
- Cellular environment: both intra and extracellular conditions can affect the activity of luciferases: pH,

TABLE II
COMPARISON BETWEEN COMMON IMAGING MODALITIES USED FOR IMAGING CANCER APPLICATIONS IN ANIMAL MODELS (ADAPTED FROM [167],[56])

Modality	FDG-PET	T2W-MRI	BLI	FLI
Operating cost	~ $5 US/time point/animal			
Equipment cost	~ $600,000	$1-2 million	< $500,000	< $500,000
Mouse preparation required	Anesthesia, tracer injection, incubation time and positioning	Anesthesia, monitoring set-up, scan before positioning	Anesthesia, tracer injection, incubation time, shaving (optional) and positioning	Anesthesia, shaving and positioning
Mouse preparation time	90 min	30 min	20 min	5 min
Scan time	15 min/3D scan	30 min/2D multislice scan/area (2 areas scanned/mouse)	1 sec – 2 min/ picture 1 – 10 pictures/scan	1 – 30 sec/ picture 1 – 10 pictures/scan
Level of knowledge for data analysis	Expert	Expert	Basic – Medium	Basic – Medium
Data analysis time	60 min	90 min	20 min	20 min
Basis for imaging	High-energy γ rays	Proton spin emission after radiowave emission	Visible light emission during chemical reaction	Visible light emission after fluorochrome excitation
Reagents used	^{18}Fluorodeoxyglucose	None	D-luciferin substrate	None
Spatial resolution	100 µm	2 mm	1 – 10 mm (depending on ROI depth)	1 – 10 mm (depending on ROI depth)
Diameter of smallest detectable tumor	< 1 mm	1 mm	< 1 mm	2 mm
Key advantages	1. Detects nonpalpable tumors 2. Relatively low background noise 3. Provides relative measures of tumor sizes 4. Has high throughput	1. Relatively high spatial resolution 2. Provides information on anatomy 3. Can localize tumors and, identify size and morphology	1. Detects nonpalpable tumors 2. Little to no background noise 3. Provides relative measures of tumor sizes 4. Has high throughput 5. Mobile equipment	1. Has high throughput 2. Mobile equipment
Key disadvantages	1. Tumor detection challenging due to high background noise in some organs	1. Has low throughput 2. Lung imaging requires expertise due to respiratory movements and high background noise	1. Detection of light emission depends on tissue depth, and local availability of co-factors and luciferins	1. Detection of light emission depends on tissue depth 2. Has high background noise due to tissue autofluorescence

temperature, and H_2O_2 concentrations can greatly affect the proper synthesis, folding, maturation, and secretion of luciferase enzymes [45]. This is particularly true for cancer applications where the conditions in the tumor environment are different from those of healthy tissues [2].

- Substrate availability and administration route: substrate availability is almost irrelevant for *in vitro* assays because in such settings the substrate is always available in excess to the enzymes. However, this factor is highly significant for *in vivo* imaging. To generate a strong *in vivo* photon emission, a sufficient amount of substrate should reach the luciferase-expressing cells and should be taken up by these cells [45]. Berger and colleagues found that the substrate exhibited a more homogeneous distribution among tissues when administered intravenously compared to intraperitoneal administration [47]. However, intraperitoneal administration yielded a prolonged organ uptake of the substrate (in this case D-luciferin). Moreover, the authors discovered that when using luciferases with glow-type reaction kinetics, such as FLuc, an incubation step of few minutes following the intraperitoneal administration permits the absorption of the substrate through the peritoneum and achieves a better distribution throughout different tissues. Whereas, for luciferases with flash type kinetics (such as GLuc and RLuc), it is best to image immediately after intravenous substrate administration to ensure the highest signal intensity [45], [47].
- Light quenching and scattering: the efficiency of bioluminescent light transmission through an animal depends largely on the type and depth of overlying tissue, as well as its scattering properties. Since, biomolecules such as hemoglobin and melanin absorb light, highly vascularized organs and highly pigmented mice tend to have lower levels of light transmission [46]. Hair and fur can also scatter and attenuate the light signal. This problem could be easily overcome by the removal of the animal's hair through depilation or shaving. However, complications may arise since hair removal can disrupt the normal hair growth cycle and subsequently change the skin pigmentation. A suggested solution to this issue was to use mice lacking a fur coat [45], [46]. As mentioned in earlier sections, the scattering and absorption of light by biological tissues is what causes BLI to have low spatial resolution.

III. BLI APPLICATIONS IN CANCER

A. *Imaging of tumorigenesis and metastasis*

Tumorigenesis is a multistep process in which cells undergo extensive mutations leading to neoplastic development [48]. Tumor cells are able to manipulate their surrounding microenvironment to promote the progression of cancer through intrinsic oncogenic pathways as well as promoting the migration of cancer cells into distal body locations, a phenomenon known as metastasis [49]. The sensitivity of BLI enables small tumor lesions to be detected at early stages of tumorigenesis that fall below the level of detection of MRI, CT, and PET imaging [50]. Typically, tumor cells are engineered *ex vivo* to express luciferase. These cells are then injected into experimental animal models and BLI is used to track tumor

growth and metastasis [39], [51]. Several *in vitro* and *in vivo* studies have been conducted in this respect. For example, Kozlowski and colleagues followed the growth of a highly metastatic human prostate cancer cell line (PC-3M) in young nude mice *in vivo* [52]. The PC-3M cells were transfected with SV40-driven modified luciferase gene to generate PC-3M-luc. Light emission was detectable within minutes of injecting the tumor cells, and continued to increase logarithmically over two weeks indicating that the bioluminescent light from the transfected cells was detectable externally and that tumor growth can be followed non-invasively. In another study, Sweeney and colleagues used BLI to monitor the growth of labeled human cervical carcinoma (HeLa) cells engrafted into immunodeficient mice [53]. They were able to obtain real-time functional data indicating spatial distributions of tumor cells at multiple times during the course of the disease. In a more recent study, Bhang and colleagues used BLI for tumor-specific imaging using progression elevated gene-3 (PEG-3) promoter driving the expression of FLuc *in vivo* [54]. Their study showed a high PEG-promoter activity in mouse models of human melanoma and breast cancer after pPEG-Luc administration. Stollfuss and colleagues conducted a study to compare the early detection abilities of PET and BLI [55]. They injected nude mice intraperitoneally with gastric cancer cells that were stably transfected with the gene coding for FLuc. Tumor development was monitored using PET and BLI after tumor cell inoculation. Upon postmortem examination, PET detected 58/82 lesions with a sensitivity of 71%, while BLI identified a total of 40/82 lesions with a sensitivity of 49%. This difference in sensitivity was attributed to light scattering and absorption as well as the site of the lesions with respect to the BLI device. The researchers found that a good correlation between BLI signal and actual tumor mass is usually observed when tumors are well-defined and close to the surface, as opposed to dispersed lesions exist deep in the body. In a study conducted by Puaux and colleagues, the practicality and performance of FDG-PET, MRI, FLI and BLI were compared for small tumor detection and tumor burden measurement using B16 tumor bearing-mice [56]. BLI and FLI were the most practical techniques with BLI and FDG-PET being able to identify small nonpalpable tumors.

Another approach that has been suggested for imaging the initiation and metastases of tumors is to monitor the release of exosomes and the microRNAs (miRNAs) found within them. These miRNAs, non-coding short RNAs, regulate different cellular and molecular pathways and are known to be mutated or abnormally expressed in the initiation and propagation stages of cancer [57]–[59]. Therefore, in a review published by Keshavarzi and colleagues, the use of BLI is suggested to detect profiling of miRNA activity to provide a clear picture of cancer proliferation and pathogenesis to help develop early detection and treatment systems for cancer [57]. BLI, as a non-invasive imaging technique, has the advantage of being able to provide a temporal pharmacodynamic profile, whereas conventional methods for miRNA profiling including Northern blotting, real-time PCR, and microarrays are invasive, unrepeatable, and time-consuming [60]. Several studies have identified diagnostic and prognostic biomarkers for this application such as miR-1280, miR-1260, miR-183, miR-200 and miR-720 for the diagnosis and staging of breast cancer [58], [61]. Liu and colleagues engineered a novel reporter gene, Luc2/tdT_miR200c_3TS, to determine the relation of miR-200 on metastasis and chemoresistance [61]. Both *in vitro* and *in vivo* studies demonstrated that high levels of miRNA expression were associated with low levels of metastases, thus can be used to measure therapeutic efficacy. In another study by Taipaleenmaki and colleagues, tumor activity and growth was monitored, *in vivo*, using BLI reporter assays to determine that miR-218-5p expression is upregulated with bone metastases found in breast cancer patients [62]. Studies such as those mentioned here indicate that modulation of miRNAs and incorporation of BLI reporters can be effectively used to provide highly sensitive and relatively quantitative imaging of molecular/cellular pathways to identify and use as diagnostic, prognostic and therapeutic biomarkers, along with development of BLI-based assays [63]–[65].

B. Imaging of cancer metabolism

Malignant tumors are endowed with intrinsic metabolic features that distinguish them from the healthy cells of whichever tissue or organ they arise in. Some of the major metabolic alterations in tumors include enhanced glucose uptake and lactate production, increased glutamine utilization and *de novo* fatty acid synthesis, as well as aberrant choline and serine metabolism. Due to this, imaging techniques are extremely valuable for performing metabolic profiling of tumors and to uncover metabolic fluctuations caused by administered treatments [66]. BLI can be used to measure ATP levels allowing for the estimation of energy levels within tumors. This is based on the fact that the reaction catalyzed by luciferase requires ATP. Thus, the amount of light emitted can be correlated to the amount of ATP available. Protocols to measure ATP levels were developed, both *in vitro* and *in vivo*, within different cellular compartments [67], [68]. The *in vitro* experiments measured ATP in the HL-1 cell line (mouse cardiac muscle cell line), while in the *in vivo* studies, human embryonic kidney cells (HEK-293) transfected with plasma membrane-targeted luciferase (pmeLUC) were used to measure the ATP concentration in the microenvironment of ovarian carcinoma tumors (OVCAR-3) and melanoma tumors (MZ2-MEL). These experiments provided three valuable pieces of information:

1. ATP concentration in the extracellular environment is very low in healthy tissues (i.e., below the threshold for HEK293-pmeLUC detection- about 1-5 μM).
2. HEK293-pmeLUC cells infiltrate ovarian carcinomas and melanomas and report ATP in the tumor microenvironment.
3. Light emission from tumors is very bright and it is close to the saturation of the luciferase signal. Thus, the intra-tumoral extracellular ATP concentration must be orders of magnitude higher than that in the healthy tissue.

Another high impact study regarding BLI of cancer metabolism was conducted by Indraccolo and Mueller-Klieser [66]. The authors used a technique known as induced metabolic bioluminescence imaging (imBLI), which is an imaging technique that enables the detection of key metabolites associated with glycolysis, such as lactate, glucose, pyruvate, and ATP in tumors. Signals captured by imBLI can be used to

visualize the topographic distribution of these metabolites and quantify their absolute amounts.

C. Imaging apoptosis

Programmed cell death or apoptosis is an important phase of the cell life cycle and a physiological process organisms utilize to prevent disease by eliminating redundant, defective, or damaged cells [5]. Cancer occurs as a result of mutations that allow cancer cells to avoid apoptosis and continue proliferating. Apoptosis occurs through the activation of intrinsic or extrinsic pathways. Both pathways require the sequential activation of zymogen cysteine proteases known as caspases. Whether apoptosis proceeds via the intrinsic or extrinsic apoptotic pathway, the activation of initiator caspases culminates in the activation of executioner caspases, such as caspase-3, whose activity results in apoptosis. Thus, monitoring caspase-3 activity permits comprehensive apoptosis detection [69]. One approach to monitor apoptosis uses an inactive luciferase reporter gene fused to a caspase-cleavage sequence. Upon caspase activation, this sequence is cleaved thereby restoring the luciferase function. Copolla and colleagues developed an apoptosis reporter using the split firefly reporter strategy where the N and C-terminals of the luciferase were fused to two strongly interacting peptides (peptide A and peptide B) [70]. This resulted in the construction of a polypeptide wherein pepA-N-Luciferase (ANLuc) and pepB-C-Luciferase (BCLuc) are positioned with an intervening caspase-3 cleavage site, which significantly reduced the bioluminescence activity of the luciferase. During apoptosis, caspase-3 cleaves the reporter, enabling the separation of ANLuc from BCLuc, and a high affinity interaction between peptide A and peptide B restores luciferase activity. This reporter system was tested using D54 cells derived from a common type of brain tumor called glioblastoma multiforme (GBM) or glioblastoma. The treatment of mice carrying D54 tumor xenografts with chemotherapeutic agents such as temozolomide and perifosine promoted apoptosis, which correlated with the activation of caspase-3 and resulted in the stimulation of bioluminescence activity. Treatment of mice with a combination therapy of temozolomide and radiation resulted in increased bioluminescence activity over individual treatments and increased therapeutic response due to enhanced apoptosis. Moreover, Scabini and colleagues described a BLI approach that uses a new formulation of Z-DEVD-aminoluciferin, a caspase 3/7 substrate, to monitor *in vivo* apoptosis in tumor cells engineered to express luciferase [71]. Using this approach, the authors were able to monitor caspase-3 activation and subsequent apoptosis induction after camptothecin and temozolomide treatments were administered to mice xenografted with colon cancer and glioblastomas tumor cells, respectively. Treated mice showed a 2-fold increase in the generation of the luminescent signal when compared to the untreated group.

D. Imaging of tumor hypoxia and angiogenesis

Since cancer cells proliferate in an uncontrolled manner with tumor cell population sizes growing at a much faster rate than normal cells, it stands to reason that their cellular respiration is also much faster. This means that not only do tumor sites require increased levels of oxygen and nutrients to survive, but they also exhibit an increased need for removal of wastes [72]. Since this task is performed by the circulatory system, the formation of neo-vasculature from pre-existing vasculature, called angiogenesis, is observed to be hyperactive at tumor sites. Angiogenesis involves four steps: stimulation of endothelial cells by growth factors, proteolytic degradation of the extracellular matrix, migration and proliferation of endothelial cells, and formation of capillary tubes [73]. Upregulated growth factors involved in angiogenesis include the vascular endothelial growth factor (VEGF) [74], [75]. Since this neovasculature has to develop fairly quickly with the rate of development of new vessel formation being slower than the rate of cell proliferation, the tumor cells at certain regions of the tumor turn hypoxic. This means that these cells undergo anaerobic respiration that results in lactic acid production, which leads to increased acidity in the tumor microenvironment [76], [77]. Hypoxia directly relates to angiogenesis in that it upregulates multiple pro-angiogenic pathways, thus influencing angiogenesis at tumor sites [78]. Measuring tumor hypoxia and angiogenesis is important as increased levels of both correlate with poor patient prognosis and increased therapy resistance [79], [80].

In 1996, Sutherland and colleagues [77] attempted to image tumor tissue taken from human cervical carcinoma biopsies and measure lactate concentrations to correlate them to hypoxia. While lactate concentrations in metastatic tumors were found to be twice those of non-metastatic samples, it was concluded that imaging times were too long, and too much tissue was required without direct information on hypoxia-levels. Therefore, it only made sense to use BLI for experimental/preclinical tumor imaging [77], [81]. Thews and colleagues conducted an experiment to measure the bioenergetic and metabolic status of tumors during radiation treatment using BLI [82]. This experiment was one of the first studies conducted *in vivo* that performed concentration-based measurements using BLI. Prior to this, typical BLI measurements were conducted *ex vivo* using tissues obtained from biopsies [83].

Recent research has demonstrated more elegant solutions to measure tumor hypoxia as opposed to measuring lactate concentrations: 1) the measurement of hypoxia-inducible factor 1 (HIF-1), a transcriptional activation factor that binds to hypoxia response element (HRE) [84]–[86]; 2) the measurement of HRE promoter activity using FLuc [87]; 3) the measurement of H_2O_2 as its increase has been linked to an increase in HIF-1 activation, therefore H_2O_2 probes can be said to play a role in hypoxia detection [88]. Van de Bittner and colleagues synthesized a bioluminescence sensitive probe for this purpose by linking Peroxy Caged Luciferin-1 (PCL-1) to aryl boronic acid, which is sensitive to H_2O_2 [89]. Upon reaction with H_2O_2, luciferin is released from the 'cage' and becomes free for the FLuc luciferase-luciferin reaction. Recently, further research has shown that this caged luciferin might favor reacting with peroxynitrite, a highly reactive oxidant that can be used for cancer imaging [90], [91]; 4) monitoring Akt kinase activity using FLuc reporter system and FLI as mitochondrial Akt accumulates during hypoxia. A split luciferase Akt reporter system (BAR) using the human NSCLC cell line (A549) is also used for imaging chemotherapeutic

responses [69], [92]. A key issue associated with BLI is that the FLuc-luciferin reaction requires oxygen for catalysis therefore, this reaction would not be ideal to image tumor hypoxic regions. Moriyama and colleagues proved that the bioluminescence signal decreases by 50% only at and below pO_2 levels of 5% and are also more ATP dependent as compared to luciferase-expression or O_2 dependents [93]. Therefore, co-factor availability should be considered for the development of innovative imaging techniques.

In the case of angiogenic imaging, a study by Heishi and colleagues imaged lymphangiogenesis and lymph node metastasis using the human breast cancer cell line, 231Luc1-cells, that expresses FLuc [94]. These cells were inoculated into the abdominal mammary fat pad of C57BL-17/Icr SCID Jcl mice and imaged after 32 days with the commercialized IVIS imaging system. These images were taken 50-60 seconds after luciferin injection. The results depicted successful decrease in lymph node metastasis in mice administered with an anti-angiogenic inhibitor, vasohibin-1. Another popular route to image angiogenesis is by using the VEGF family of signaling proteins (i.e., imaging dependent on protein expression and not bioluminescence signals). Some ways that have been used to develop *in vivo* bioluminescence assays using the VEGF family of signaling proteins include VEGF gene expression and levels [51] [22], VEGF receptor expression [95], imaging using αvβ3 expression or probes [96], and the Apelin-Apj ligand-receptor pair [97].

IV. Imaging of Response to Cancer Treatments

There is a wide range of identified mechanisms to drug resistance in the field of chemotherapeutics. Most of the failures of chemotherapeutic treatments and cancer recurrences are due to the development of drug resistance. Mansoori and colleagues provided a brief review on these mechanisms [98]. A study conducted by Yu and colleagues used a pcDNA3-Luc vector [99], a FLuc reporter vector, optimized for mammalian expression [85]. It was transfected into T47D, TYS clone-4 and TDG clone-1 cells to study the Myc overexpression in estrogen receptor α (ERα) mutations. This was done due to their correlation to endocrine therapy resistance in metastatic breast cancers. Such studies demonstrate the important role of BLI in the field of cancer research.

Accurate therapeutic evaluation of developed chemotherapeutic agents, immunotherapeutic agents, and radiotherapy strategies are essential in the scheme of cancer treatment. Traditionally, therapeutic efficacy is gaged by measuring tumor size, performing histological analyses of the tumor, and assessing the overall survival rate. In the last two decades genetically modified animal models (GEM) have contributed tremendously to the understanding of the molecular mechanisms, identification of new therapeutic targets, and preclinical evaluation of drugs. Cancer therapy murine models of subcutaneously implanted tumors provide a powerful test system for evaluating the therapeutic efficacy of antineoplastics [2], [100]. Molecular imaging modalities coupled with GEMs have revolutionized the field of drug discovery and its evaluation in preclinical settings.

A. BLI of response to chemotherapy

Chemotherapy is a type of cancer treatment that uses one or more anti-cancer drugs. The main issue with chemotherapy is that the drugs have adverse side effects that can greatly reduce the quality of life of cancer patients. These side effects however can be minimized by the careful selection of suitable chemotherapeutic agents and the determination of the optimum dosage needed in clinical applications. Tumor cells expressing bioluminescent reporters can be used as metabolic indicators for the preclinical evaluation of therapeutic response. In such evaluations, it is assumed that apoptosis and cell death induced by anti-cancer drugs provides a lower expression of luciferase protein. This indirectly reveals the metabolic rate of the tumor and can be directly correlated with the cell-killing effect of anti-cancer agents [2]. In a survey of relevant studies, Li and colleagues developed an orthotropic lung cancer model in which luciferase expressing human lung adenocarcinoma (A549) cancer cells were injected into athymic nude mice [101]. Next, the mice were treated with 30 mg/kg paclitaxel and the tumor growth overtime was monitored using BLI. The response to paclitaxel was seen as a decrease in bioluminescence, which indicated cell death. In another study, Viola and colleagues used BLI to noninvasively image the upregulation of hypoxia-inducible factor 1 (HIF-1) *in vivo* after the administration of chemotherapy [102]. Results of studies on radiotherapy have indicated that HIF-1 is a protein that plays an important role in tumor resistance to radiotherapy. Accordingly, the authors hypothesized that BLI could be used to depict the increase in HIF-1 levels in tumors after chemotherapy administration. With both radiotherapy and chemotherapy, an increase in HIF-1 levels is associated with the elicitation of a cytotoxic effect that kills tumor cells.

B. BLI of response to radiotherapy

Radiotherapy is a cancer treatment strategy used when the tumors have not metastasized and are instead localized in one discrete location of the body. Like all other conventional cancer therapies, radiotherapy can lead to unwanted side effects. Thus, preclinical evaluation of radiation treatment is essential to optimize the dose and exposure time needed for achieving the desired treatment [2]. For example, radiotherapy used in the treatment of pediatric musculoskeletal sarcomas can result in crippling defects of skeletal growth. Several protective strategies have shown potential in preserving the growth function of the irradiated epiphyses, but most have not been evaluated in tumor-bearing animal models. Horton and colleagues used two bioluminescent human rhabdomyosarcoma cell lines to establish xenograft tumors in skeletally immature mice [103]. BLI allowed the continuous evaluation of tumor growth and tibial elongation following localized radiotherapy. It was observed that mice receiving high-dose (10Gray) radiotherapy experienced reduced tumor growth velocity and a prolonged median of survival, but the treatment also resulted in a significant (~3%) shortening of the irradiated limb. Whereas, the second group of mice exposed to a lower dose (2Gy) resulted in 4.1% decrease in limb length but did not extend survival. Moreover, Zhang and colleagues developed a BLT system to guide radiotherapy [104]. The authors first conducted phantom studies using tissue simulating

phantoms and mice carcasses to assess the BLT's targeting accuracy. Their second set of experiments involved using their developed BLT system to image a group of mice implanted with a light source as well as another group bearing subcutaneous tumors xenografted from firefly PC3-Luc prostate cancer cell line. The optical system was found capable of locating targets with an average accuracy of 1 mm, which provided an effective solution for soft tissue targeting, particularly for small, non-palpable, or orthotropic tumor models.

C. BLI of response to immunotherapy

Immunotherapy is a cancer treatment modality that uses the patient's immune system to fight cancer. Employing the patient's immune system could either be through stimulating the immune system to work harder or smarter to attack cancer cells, or by giving the patient immune system components such as man-made immune system proteins [105]. For instance, one of the principal treatment modalities within the field of cancer immunotherapy is adoptive T cell therapy (ACT). This method involves expanding patient-derived T cells specific for tumor-associated antigens (TAA) outside the patient's body then re-infusing them into the bloodstream to target and destroy cancer cells [106]. Immunotherapy is regarded as a valuable therapeutic approach, in this context, pharmacologic agents with immunomodulating properties are being developed for cancer treatment. With respect to BLI applications in monitoring response to immunotherapy, Rozemuller and colleagues injected tumors from seven multiple myeloma cell lines transfected with a green fluorescent protein FLuc fusion gene into RAG2 knockout mice [107]. Established tumors were treated with radiotherapy or with allogeneic peripheral blood mononuclear cell infusions. Tumors treated with radiotherapy showed temporary regression. However, infusion of allogeneic peripheral blood mononuclear cells resulted in the complete eradication of tumors. Moreover, these experiments demonstrated that tumor regression and progression could be easily and sensitively monitored using BLI. Maes and colleagues investigated the value of BLI in the context of dendritic cell (DC) immunotherapy [108]. Mice were injected with GL261 glioma cells transfected with D-luciferase and BLI was studied as an imaging tool in the context of immunotherapy against malignant glioma. In order to prove that the *in vivo* BLI signal is an adequate measure of the luciferase activity in the GL261 glioma model, the authors correlated the *in vivo* BLI signal with *ex vivo* BLI values obtained from brain slices and *in vitro* luminometric measurements. Linear regression analyses revealed a strong linear correlation between *in vivo* and *ex vivo* BLI, as well as, a strong linear correlation between *ex vivo* BLI and *in vitro* luciferase activity measurements.

D. BLI of response to gene therapy

A statistical study of gene therapy shows that 65% of all gene therapy trials up to 2017 were attributed to cancer gene therapy and there was a steady increase in gene therapy trials since 2012 [109]. Due to the recent development of the first FDA-approved gene therapy treatment involving CAR-T therapy, preclinical testing in this area shall be essential for clinical translation of other gene therapies [110]. Gene therapy refers to the process of modifying genetic material and by extension, modifying cells to cure or treat cancer [111]. Imaging techniques associated with gene therapy are of two types; transduction and biodistribution imaging. Transduction imaging methods could detect transgene-mediated protein production, whereas biodistribution-imaging methods could track gene delivery vectors [112], [113]. This involves imaging the expression of the therapeutic gene after it has been transferred to evaluate the efficiency of the treatment [13], [113]. Several studies in gene therapy have been conducted to monitor tumor phenomena using BLI including the imaging of metastasis [114], apoptosis [115], [116], tumor hypoxia [117]–[122], and angiogenesis [123].

As indicated earlier in this paper, imaging of exosomes and more specifically, miRNAs using BLI has proven to be invaluable in measuring the efficacy of miRNA-based therapy targeted at various tumor-related phenomenon [124]–[126]. In a review by Sekar and colleagues, a summary is presented on the miRNAs that play a part in oncogenic factor expression and their downstream targets and how BLI assays can be used to monitor their expression and their use as therapeutic targets [125]. Several studies involving overexpression of anti-oncogenic miRNAs have used BLI reporter systems to accurately identify the effect of this targeted therapy [127]–[134]. In the field of oncology, BLI reporters have been or can be used to measure the downregulation or upregulation of miRNA to detect tumor growth and spread and to assess miRNA delivery activity to specific targets. These targets could be used to inhibit expression of certain factors, and to measure viral vectors activity for therapeutic treatment. The specificity and the ability of BLI to monitor different target activities within the same *in vivo* system makes it a powerful tool for imaging in current gene therapy trials.

E. BLI of response to stem cell therapy

Imaging using stem cells has vast potential in the study of cancer. Stem cells can differentiate into different lineages and imaging techniques focus on their location, viability, self and surrounding tissue interactions, as well as their number and protein expression levels. There are different types of stem cells including blastocyst-derived embryonic stem cells (ESCs), mesenchymal stem cells (MSCs), adult human derived bone marrow stem cells (BMSCs) and adult cells reprogrammed via transfection called induced pluripotent stem cells (iPSC) [135], [136]. In imaging applications, stem cells labeled with luciferase are engrafted *in vivo* and monitored for transgene expression or/and therapy response. Since BLI uses genetic labeling for luciferase expression, it has the capability to image the viability and differentiation states of these cells. In terms of therapy, cells can be used to express drugs; specifically MSCs whose natural tropism for tumor sites makes them excellent vehicles for tumor-targeted therapies [13] [137]. Hepatocellular carcinomas are known to be resistant to drugs, and thus, Yang and colleagues targeted these drug resistant cancer stem cells (HCC CSCs) by loading Bmi1 siRNA (Bmi1siR) into cisplatin nanocapsules in mice [138]. The Bmi1siR would inhibit the expression of Bmi1 proteins, which are crucial for the survival and proliferation of HCC CSCs. In another study, the metastasis of triple negative breast cancer cells (TNBC) was reduced by

decreasing the CSC-like properties found in TNBC cells. LM2 cells transfected with a pMirTarget vector with FLuc reporter gene were used, this reduced TBNC metastasis by down regulating the α5 integrin [139]–[141]. Numerous other studies targeting breast CSCs [142]–[145], brain CSCs [146], [147], and others using SCs [148] have been conducted recently. Within the field of genetic-modification for the expression of therapeutic molecules, a high impact study by Yin and colleagues solved the inherent problem of these molecules releasing drugs at non-specific sites, causing hepatotoxicity [149]. They did this by delivering activating genes to 'turn on' the therapeutic gene expression of the modified CSCs. Specifically, they engineered adipose-derived MSCs that would express tumor necrosis factor-related apoptosis inducing ligand (TRAIL), and activated their expression by mild magnetic hyperthermia-activated secretion of TRAIL using synthesized nanoparticles. BLI was employed by injecting luciferase-transfected human ovarian cancer cells (A2780) into mice, and the tumor volume was imaged in response to therapy treatment.

Finally, Fig. 8 presents a visual representation of the distribution of literature with respect to each of the aforementioned BLI cancer applications. Moreover, Table III and Table IV provide a summary of the studies relating to the applications of BLI in cancer imaging discussed in this paper.

V. Conclusion

BLI is a powerful imaging modality that has been developed over the last decade as a tool for studying ongoing biological processes *in vivo*. This form of optical imaging is low cost and noninvasive and facilitates real-time analysis of disease processes at the molecular level in living organisms. This paper provided a comprehensive review of BLI in the preclinical therapeutic evaluation of tumors, as well as examples on how this imaging strategy can accelerate drug development and the evaluation of tumor response to cancer therapy.

VI. Abbreviations

ACT	Adoptive T-cell Therapy
ANLuc	pepA-N-Luciferase
BCLuc	pepB-C-Luciferase
BLI	Bioluminescence Imaging
BLT	Bioluminescence Tomography
CCD	Charged Coupled Device
CNR	Contrast-to-Noise Ratio
CT	Computed Tomography
CSC	Cancer stem cells
DC	Dendritic Cell
FDG	Fluorodeoxyglucose
FLI	Fluorescence Imaging
FLuc	Firefly Luciferase
FOV	Field of View
GBM	Glioblastoma Multiforme
GEM	Genetically Modified Animal Models
GLuc	*Gaussia* Luciferase
HeLa	Human Cervical Cancer Cell Line
HL-1	Mouse Cardiac Muscle Cell Line
HEK-293	Human Embryonic Kidney Cell Line
HNSCC	Head and Neck Squamous Cell Carcinoma

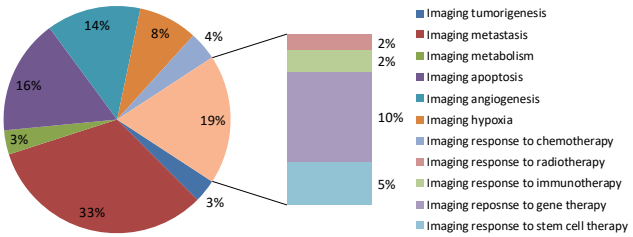

Fig. 8. Distribution of citations for cancer applications in BLI (Data obtained from the Web of Science).

HIF-1	Hypoxia Inducible Factor 1
imBLI	Induced Metabolic Bioluminescence Imaging
miRNA	microRNA
MDA-MB-231	Human Breast Cancer Cell Line
MRI	Magnetic Resonance Imaging
MZ2-Mel	Melanoma Cell Line
NLuc	NanoLuc Luciferase
OVCAR 3	Ovarian Cancer Cell Line
PC-3M	Human Prostate Cancer Cell Line
PET	Positron Emission Tomography
PEG 3	Progression Elevated Gene 3
pmeLUC	Plasma Membrane-targeted Luciferase
RLU	Relative Light Unit
RLuc	*Renilla* Luciferase
RTE	Radiative Transfer Equation
SPECT	Single Photon Emission Tomography
SNR	Signal-to-Noise Ratio
TAA	Tumor Associated Antigens
US	Ultrasound
VLuc	*Vargula* Luciferase

References

[1] F. Bray, J. Ferlay, I. Soerjomataram, R. L. Siegel, L. A. Torre, and A. Jemal, "Global cancer statistics 2018: GLOBOCAN estimates of incidence and mortality worldwide for 36 cancers in 185 countries," *CA. Cancer J. Clin.*, vol. 68, no. 6, pp. 394–424, Sep. 2018, doi: 10.3322/caac.21492.

[2] T. V. Sekar and R. Paulmurugan, "Bioluminescence Imaging of Cancer Therapy," in *Cancer Theranostics*, X. Chen and S. T. C. Wong, Eds. California: Elsevier Inc., 2014, pp. 69–93.

[3] H. Mirzaei *et al.*, "Boron neutron capture therapy: Moving toward targeted cancer therapy," *Journal of Cancer Research and Therapeutics*, vol. 12, no. 2. Medknow Publications, pp. 520–525, 01-Apr-2016, doi: 10.4103/0973-1482.176167.

[4] M. H. Michalski and X. Chen, "Molecular imaging in cancer treatment," *European Journal of Nuclear Medicine and Molecular Imaging*, vol. 38, no. 2. pp. 358–377, 2011, doi: 10.1007/s00259-010-1569-z.

[5] O. Gheysens and F. M. Mottaghy, "Method of bioluminescence imaging for molecular imaging of physiological and pathological processes," *Methods*, vol. 48, no. 2, pp. 139–145, Jun. 2009, doi: 10.1016/j.ymeth.2009.03.013.

[6] M. F. Kircher, H. Hricak, and S. M. Larson, "Molecular imaging for personalized cancer care," *Mol. Oncol.*, vol. 6, no. 2, pp. 182–195, Apr. 2012, doi: 10.1016/J.MOLONC.2012.02.005.

[7] T. Hussain and Q. T. Nguyen, "Molecular Imaging for Cancer Diagnosis and Surgery HHS Public Access," *Adv Drug Deliv Rev*, vol. 66, pp. 90–100, 2014, doi: 10.1016/j.addr.2013.09.007.

[8] J. E. Lloyd and E. C. Gentry, "Bioluminescence," in *Encyclopedia of Insects*, Academic Press, 2009, pp. 101–105.

[9] S. Sharifian, A. Homaei, R. Hemmati, R. B Luwor, and K. Khajeh, "The emerging use of bioluminescence in medical research.," *Biomed. Pharmacother.*, vol. 101, pp. 74–86, May 2018, doi: 10.1016/j.biopha.2018.02.065.

[10] J. W. Hastings, "Chemistries and colors of bioluminescent reactions: a review," *Gene*, vol. 173, no. 1, pp. 5–11, 1996, doi: https://doi.org/10.1016/0378-1119(95)00676-1.

[11] S. Lyons, P. S. Patrick, and K. Brindle, "Imaging Mouse Cancer Models In Vivo Using Reporter Transgenes," *Cold Spring Harb. Lab. Press*, vol. 8, pp. 685–699, 2013, doi: doi:10.1101/pdb.top069864.

[12] S. Iwano *et al.*, "Single-cell bioluminescence imaging of deep tissue in freely moving animals," *Science*, vol. 359, no. 6378, pp. 935–939, Feb. 2018, doi: 10.1126/science.aaq1067.

[13] C. E. Badr and B. A. Tannous, "Bioluminescence imaging: progress and applications," *Trends Biotechnol.*, vol. 29, no. 12, pp. 624–633, 2011, doi: 10.1016/j.tibtech.2011.06.010.

[14] S. K. Lyons, "Bioluminescence Imaging," *Encyclopedia of Cancer*. Springer Berlin Heidelberg, Berlin, Heidelberg, pp. 405–408, 2011, doi: 10.1007/978-3-642-16483-5_640.

[15] D. M. Connor and A. M. Broome, "Gold Nanoparticles for the Delivery of Cancer Therapeutics," in *Advances in Cancer Research*, vol. 139, A. M. Broome, Ed. Academic Press, 2018, pp. 163–184.

[16] K. E. Luker and D. B. T. Piwnica-Worms, "Optimizing Luciferase Protein Fragment Complementation for Bioluminescent Imaging of Protein–Protein Interactions in Live Cells and Animals," *Methods Enzymol.*, vol. 385, pp. 349–360, 2004, doi: https://doi.org/10.1016/S0076-6879(04)85019-5.

[17] T. Noguchi and S. Golden, "Bioluminescent and fluorescent reporters in circadian rhythm studies," *Bioclock Stud.*, pp. 1–24, 2017.

[18] Y. Nakajima and Y. Ohmiya, "Bioluminescence assays: multicolor luciferase assay, secreted luciferase assay and imaging luciferase assay," *Expert Opin. Drug Discov.*, vol. 5, no. 9, pp. 835–849, 2010, doi: 10.1517/17460441.2010.506213.

[19] C. Badr, "Bioluminescence Imaging: Basics and Practical Limitations," in *Bioluminescent Imaging*, vol. 1098, Clifton, New Jersey: Humana Press Inc., 2014, pp. 1–18.

[20] S. H. D. Haddock, M. A. Moline, and J. F. Case, "Bioluminescence in the Sea," *Ann. Rev. Mar. Sci.*, vol. 2, no. 1, pp. 443–493, Dec. 2009, doi: 10.1146/annurev-marine-120308-081028.

[21] Thermo Fisher Scientific, "Luciferase Reporters," *Thermofisher.com*, 2018. [Online]. Available: https://www.thermofisher.com/ae/en/home/life-science/protein-biology/protein-biology-learning-center/protein-biology-resource-library/pierce-protein-methods/luciferase-reporters.html. [Accessed: 06-Dec-2018].

[22] Promega, "Reporter Vectors," *Worldwide.promega.com*. [Online]. Available: https://worldwide.promega.com/resources/vector-sequences/reporter-vectors/. [Accessed: 04-Dec-2018].

[23] Promega, "Luciferase Assay System," *Worldwide.promega.com*, 2018. [Online]. Available: https://worldwide.promega.com/products/reporter-assays-and-transfection/reporter-assays/luciferase-assay-system/?catNum=E1500. [Accessed: 07-Dec-2018].

[24] T. Xu, D. Close, W. Handagama, E. Marr, G. Sayler, and S. Ripp, "The Expanding Toolbox of In Vivo Bioluminescent Imaging," *Front. Oncol.*, vol. 6, no. 150, 2016, doi: 10.3389/fonc.2016.00150.

[25] T. Kuchimaru *et al.*, "A luciferin analogue generating near-infrared bioluminescence achieves highly sensitive deep-tissue imaging," *Nat. Commun.*, vol. 7, 2016, doi: 10.1038/ncomms11856.

[26] Y. Nasu and R. E. Campbell, "Unnaturally aglow with a bright inner light," *Science*, vol. 359, no. 6378, pp. 868–869, 2018, doi: 10.1126/science.aas9159.

[27] J. M. M. Leitão and J. C. G. Esteves da Silva, "Firefly luciferase inhibition," *J. Photochem. Photobiol. B Biol.*, vol. 101, no. 1, pp. 1–8, 2010, doi: 10.1016/j.jphotobiol.2010.06.015.

[28] M. Keyaerts *et al.*, "Plasma protein binding of luciferase substrates influences sensitivity and accuracy of bioluminescence imaging," *Mol. Imaging Biol.*, vol. 13, no. 1, pp. 59–66, 2011, doi: 10.1007/s11307-010-0325-x.

[29] Perkin Elmer, "IVIS Spectrum Preclinical in vivo imaging." [Online]. Available: https://www.perkinelmer.com/lab-solutions/resources/docs/BRO_010572B_01_PRD_IVIS_Spectrum.pdf. [Accessed: 07-Dec-2018].

[30] "New Products," *Science*, vol. 306, no. 5693, pp. 133 LP – 133, Oct. 2004, doi: 10.1126/science.306.5693.133.

[31] M. Lewis *et al.*, "A Multi-Camera System for Bioluminescence Tomography in Preclinical Oncology Research," *Diagnostics*, vol. 3, no. 3, pp. 325–343, 2013, doi: 10.3390/doi:10.3390/diagnostics3030325.

[32] K. R. Zinn *et al.*, "Noninvasive bioluminescence imaging in small animals," *ILAR J.*, vol. 49, no. 1, pp. 103–115, 2008, doi: 10.1093/ilar.49.1.103.

[33] G. Wang *et al.*, "Recent development in bioluminescence tomography," in *3rd IEEE International Symposium on Biomedical Imaging: Nano to Macro*, 2006, pp. 678–681, doi: 10.1109/ISBI.2006.1625007.

[34] J. A. Guggenheim, H. R. A. Basevi, J. Frampton, I. B. Styles, and H. Dehghani, "Multi-modal molecular diffuse optical tomography system for small animal imaging," *Meas. Sci. Technol.*, vol. 24, no. 10, 2013, doi: 10.1088/0957-0233/24/10/105405.

[35] Y. Ando *et al.*, "In vivo bioluminescence and reflectance imaging of multiple organs in bioluminescence reporter mice by bundled-fiber-coupled microscopy," *Biomed. Opt. Express*, vol. 7, no. 3, pp. 963–978, 2016, doi: 10.1364/BOE.7.000963.

[36] J. C. Tseng, K. Vasquez, and J. D. Peterson, "Optical Imaging on the IVIS Spectrum CT System: General and Technical Considerations for 2D and 3D Imaging," *PerkinElmer technical note*, 2015. [Online]. Available: https://www.perkinelmer.com/CMSResources/Images/44-171013TCH_012007_01_IVIS-2D_3D_Imaging.pdf. [Accessed: 08-Dec-2018].

[37] S. Mollard, R. Fanciullino, S. Giacometti, C. Serdjebi, S. Benzekry, and J. Ciccolini, "In Vivo Bioluminescence Tomography for Monitoring Breast Tumor Growth and Metastatic Spreading: Comparative Study and Mathematical Modeling," *Sci. Rep.*, vol. 6, 2016, doi: 10.1038/srep36173.

[38] W. Han and G. Wang, "Bioluminescence Tomography: Biomedical Background, Mathematical Theory, and Numerical Approximation.," *J. Comput. Math.*, vol. 26, no. 3, pp. 324–335, 2008.

[39] R. T. Sadikot and T. S. Blackwell, "Bioluminescence Imaging," *Proc. Am. Thorac. Soc.*, vol. 2, no. 6, pp. 537–540, 2005, doi: 10.1513/pats.200507-067DS.

[40] L. Mezzanotte, M. van 't Root, H. Karatas, E. A. Goun, and C. W. G. M. Löwik, "In Vivo Molecular Bioluminescence Imaging: New Tools and Applications," *Trends Biotechnol.*, vol. 35, no. 7, pp. 640–652, Jul. 2017, doi: 10.1016/j.tibtech.2017.03.012.

[41] C. Darne, Y. Lu, and E. M. Sevick-Muraca, "Small animal fluorescence and bioluminescence tomography: A review of approaches, algorithms and technology update," *Phys. Med. Biol.*, vol. 59, no. 1, 2014, doi: 10.1088/0031-9155/59/1/R1.

[42] M. Jiang, T. Zhou, J. Cheng, W. Cong, and G. Wang, "Image reconstruction for bioluminescence tomography from partial measurement.," *Opt. Express*, vol. 15, no. 18, pp. 11095–11116, Sep. 2007.

[43] N. V Slavine and R. W. McColl, "Semi-automated Image Processing for Preclinical Bioluminescent Imaging.," *J. Appl. Bioinforma. Comput. Biol.*, vol. 4, no. 1, p. 114, 2015, doi: 10.4172/2329-9533.1000114.

[44] X. Pennec, "Introduction to Medical Imaging MVA 2011-2012," *Image Processing*. Cambridge University Press, Cambridge, pp. 1–15, 2012, doi: 10.1017/CBO9780511760976.

[45] C. E. Badr, *Bioluminescent Imaging*, vol. 1098. 2014.

[46] K. O'neill, S. K. Lyons, W. M. Gallagher, K. M. Curran, and A. T. Byrne, "Bioluminescent imaging: a critical tool in pre-clinical oncology research," *J. Pathol. J Pathol*, vol. 220, pp. 317–327, 2010, doi: 10.1002/path.2656.

[47] F. Berger, R. Paulmurugan, S. Bhaumik, and S. S. S. Gambhir, "Uptake kinetics and biodistribution of 14C-d-luciferin-a radiolabeled substrate for the firefly luciferase catalyzed bioluminescence reaction: Impact on bioluminescence based reporter gene imaging," *Eur. J. Nucl. Med. Mol. Imaging*, vol. 35, no. 12, pp. 2275–2285, Dec. 2008, doi: 10.1007/s00259-008-0870-6.

[48] R. Ashkenazi, S. N. Gentry, and T. L. Jackson, "Pathways to tumorigenesis-modeling mutation acquisition in stem cells and their progeny," *Neoplasia*, vol. 10, no. 11, pp. 1170–1182, Nov. 2008.

[49] B. Kocher and D. Piwnica-Worms, "Illuminating cancer systems with genetically engineered mouse models and coupled luciferase reporters in vivo.," *Cancer Discov.*, vol. 3, no. 6, pp. 616–29, Jun. 2013, doi: 10.1158/2159-8290.CD-12-0503.

[50] M. Momcilovic and D. B. Shackelford, "Imaging Cancer Metabolism.," *Biomol. Ther.* , vol. 26, no. 1, pp. 81–92, Jan. 2018, doi: 10.4062/biomolther.2017.220.

[51] M. Edinger, T. J. Sweeney, A. A. Tucker, A. B. Olomu, R. S. Negrin, and C. H. Contag, "Noninvasive assessment of tumor cell proliferation in animal models.," *Neoplasia*, vol. 1, no. 4, pp. 303–310, Oct. 1999.

[52] J. M. Kozlowski, I. J. Fidler, D. Campbell, Z. L. Xu, M. E. Kaighn, and I. R. Hart, "Metastatic Behavior of Human Tumor Cell Lines Grown in

the Nude Mouse1," *Cancer Res.*, vol. 44, pp. 3522–3529, 1984.

[53] T. J. Sweeney *et al.*, "Visualizing the kinetics of tumor-cell clearance in living animals.," *Proc. Natl. Acad. Sci. U. S. A.*, vol. 96, no. 21, pp. 12044–9, Oct. 1999.

[54] H. C. Bhang, K. L. Gabrielson, J. Laterra, P. B. Fisher, and M. G. Pomper, "Tumor-specific imaging through progression elevated gene-3 promoter-driven gene expression.," *Nat. Med.*, vol. 17, no. 1, pp. 123–9, Jan. 2011, doi: 10.1038/nm.2269.

[55] J. Stollfuss *et al.*, "Non-invasive imaging of implanted peritoneal carcinomatosis in mice using PET and bioluminescence imaging.," *EJNMMI Res.*, vol. 5, no. 1, p. 125, Dec. 2015, doi: 10.1186/s13550-015-0125-z.

[56] A. L. Puaux *et al.*, "A comparison of imaging techniques to monitor tumor growth and cancer progression in living animals.," *Int. J. Mol. Imaging*, vol. 2011, p. 321538, Nov. 2011, doi: 10.1155/2011/321538.

[57] M. Keshavarzi *et al.*, "MicroRNAs-Based Imaging Techniques in Cancer Diagnosis and Therapy," *J. Cell. Biochem.*, vol. 118, no. 12, pp. 4121–4128, Dec. 2017, doi: 10.1002/jcb.26012.

[58] S. H. Jafari *et al.*, "Breast cancer diagnosis: Imaging techniques and biochemical markers," *Journal of Cellular Physiology*, vol. 233, no. 7. Wiley-Liss Inc., pp. 5200–5213, 01-Jul-2018, doi: 10.1002/jcp.26379.

[59] L. M. Shen, L. Quan, and J. Liu, "Tracking Exosomes in Vitro and in Vivo to Elucidate Their Physiological Functions: Implications for Diagnostic and Therapeutic Nanocarriers," *ACS Appl. Nano Mater.*, vol. 1, no. 6, pp. 2438–2448, 2018, doi: 10.1021/acsanm.8b00601.

[60] S. W. Oh, D. W. Hwang, and D. S. Lee, "In vivo monitoring of microRNA biogenesis using reporter gene imaging," *Theranostics*, vol. 3, no. 12, pp. 1004–1011, 2013, doi: 10.7150/thno.4580.

[61] H. Liu *et al.*, "Roles of miRNAs in breast cancer stem cells, drug sensitivity, and spontaneous metastases in orthotopic human-in-mouse models.," *J. Clin. Oncol.*, vol. 29, pp. 1082–1082, 2011, doi: 10.1200/jco.2011.29.15_suppl.1082.

[62] H. Taipaleenmäki *et al.*, "miR-218-Wnt signaling promotes breast cancer-induced osteolytic disease," *Osteologie*, vol. 7, no. 48, pp. 79032–79046, 2016.

[63] K. A. Cissell, Y. Rahimi, S. Shrestha, E. A. Hunt, and S. K. Deo, "Bioluminescence-based detection of microRNA, miR21 in breast cancer cells," *Anal. Chem.*, vol. 80, no. 7, pp. 2319–2325, 2008, doi: 10.1021/ac702577a.

[64] F. Wang *et al.*, "Noninvasive Visualization of MicroRNA-16 in the Chemoresistance of Gastric Cancer Using a Dual Reporter Gene Imaging System," *PLoS One*, vol. 8, no. 4, p. e61792, 2013, doi: 10.1371/journal.pone.0061792.

[65] H. Mirzaei *et al.*, "The therapeutic potential of human adipose-derived mesenchymal stem cells producing CXCL10 in a mouse melanoma lung metastasis model," *Cancer Lett.*, vol. 419, pp. 30–39, Apr. 2018, doi: 10.1016/j.canlet.2018.01.029.

[66] S. Indraccolo and W. Mueller-Klieser, "Potential of Induced Metabolic Bioluminescence Imaging to Uncover Metabolic Effects of Antiangiogenic Therapy in Tumors.," *Front. Oncol.*, vol. 6, p. 15, 2016, doi: 10.3389/fonc.2016.00015.

[67] G. Morciano *et al.*, "Use of luciferase probes to measure ATP in living cells and animals," *Nat. Protoc.*, vol. 12, no. 8, pp. 1542–1562, 2017, doi: 10.1038/nprot.2017.052.

[68] P. Pellegatti, L. Raffaghello, G. Bianchi, F. Piccardi, V. Pistoia, and F. Di Virgilio, "Increased level of extracellular ATP at tumor sites: in vivo imaging with plasma membrane luciferase.," *PLoS One*, vol. 3, no. 7, p. e2599, Jul. 2008, doi: 10.1371/journal.pone.0002599.

[69] K. Suchowski, T. Pöschinger, A. Rehemtulla, M. Stürzl, and W. Scheuer, "Noninvasive Bioluminescence Imaging of AKT Kinase Activity in Subcutaneous and Orthotopic NSCLC Xenografts: Correlation of AKT Activity with Tumor Growth Kinetics," *Neoplasia*, vol. 19, no. 4, pp. 310–320, 2017, doi: 10.1016/j.neo.2017.02.005.

[70] J. M. Coppola, B. D. Ross, and A. Rehemtulla, "Noninvasive imaging of apoptosis and its application in cancer therapeutics.," *Clin. Cancer Res.*, vol. 14, no. 8, pp. 2492–501, Apr. 2008, doi: 10.1158/1078-0432.CCR-07-0782.

[71] M. Scabini, F. Stellari, P. Cappella, S. Rizzitano, G. Texido, and E. Pesenti, "In vivo imaging of early stage apoptosis by measuring real-time caspase-3/7 activation," *Apoptosis*, vol. 16, no. 2, pp. 198–207, 2011, doi: 10.1007/s10495-010-0553-1.

[72] D. Hanahan and R. A. Weinberg, "The Hallmarks of Cancer," *Cell*, vol. 100, no. 1, pp. 57–70, 2000, doi: 10.1016/S0092-8674(00)81683-9.

[73] N. H. Goradel *et al.*, "Nanoparticles as new tools for inhibition of cancer angiogenesis," *Journal of Cellular Physiology*, vol. 233, no. 4. Wiley-Liss Inc., pp. 2902–2910, 01-Apr-2018, doi: 10.1002/jcp.26029.

[74] Y. Maeshima, "Angiogenesis and Cancer," in *Apoptosis, Cell Signaling, and Human Diseases: Molecular mechanisms*, R. Srivastava, Ed. Humana Press, 2007, pp. 35–61.

[75] B. A. Bryan and P. A. D'Amore, "What tangled webs they weave: Rho-GTPase control of angiogenesis," *Cell. Mol. Life Sci.*, vol. 64, no. 16, pp. 2053–2065, 2007, doi: 10.1007/s00018-007-7008-z.

[76] F. Danhier, O. Feron, and V. Préat, "To exploit the tumor microenvironment: Passive and active tumor targeting of nanocarriers for anti-cancer drug delivery," *J. Control. Release*, vol. 148, no. 2, pp. 135–146, 2010, doi: 10.1016/j.jconrel.2010.08.027.

[77] R. M. Sutherland, W. A. Ausserer, B. J. Murphy, and R. R. Laderoute, "Tumor hypoxia and heterogeneity: Challenges and opportunities for the future," *Semin. Radiat. Oncol.*, vol. 6, no. 1, pp. 59–70, 1996, doi: https://doi.org/10.1016/S1053-4296(96)80036-1.

[78] B. L. Krock, N. Skuli, and M. C. Simon, "Hypoxia-induced angiogenesis: good and evil," *Genes Cancer*, vol. 2, no. 12, pp. 1117–1133, Dec. 2011, doi: 10.1177/1947601911423654.

[79] J. C. Walsh, A. Lebedev, E. Aten, K. Madsen, L. Marciano, and H. C. Kolb, "The Clinical Importance of Assessing Tumor Hypoxia : Relationship of Tumor Hypoxia to Prognosis," *Antioxidants Redox Signal.*, vol. 21, no. 10, pp. 1516–1554, 2014, doi: 10.1089/ars.2013.5378.

[80] V. Askoxylakis *et al.*, "Investigation of tumor hypoxia using a two-enzyme system for in vitro generation of oxygen deficiency," *Radiat. Oncol.*, 2011, doi: 10.1186/1748-717X-6-35.

[81] J. A. Raleigh, M. W. Dewhirst, and D. E. Thrall, "Measuring tumor hypoxia," *Semin. Radiat. Oncol.*, vol. 6, no. 1, pp. 37–45, 1996, doi: 10.1016/S1053-4296(96)80034-8.

[82] O. Thews, F. Zywietz, B. Lecher, and P. Vaupel, "Quantitative changes of metabolic and bioenergetic parameters in experimental tumors during fractionated irradiation," *Int. J. Radiat. Oncol.*, vol. 45, no. 5, pp. 1281–1288, 1999, doi: https://doi.org/10.1016/S0360-3016(99)00263-1.

[83] S. Walenta, T. Schroeder, and W. Mueller-Klieser, "Metabolic mapping with bioluminescence: Basic and clinical relevance," *Biomol. Eng.*, vol. 18, no. 6, pp. 249–262, 2002, doi: 10.1016/S1389-0344(01)00107-1.

[84] S. J. Goldman *et al.*, "Use of the ODD-luciferase transgene for the non-invasive imaging of spontaneous tumors in mice," *PLoS One*, vol. 6, no. 3, p. e18269, 2011, doi: 10.1371/journal.pone.0018269.

[85] M. Safran *et al.*, "Mouse model for noninvasive imaging of HIF prolyl hydroxylase activity: Assessment of an oral agent that stimulates erythropoietin production," *Proc. Natl. Acad. Sci.*, vol. 103, no. 1, pp. 105–110, 2006, doi: 10.1073/pnas.0509459103.

[86] P. Iglesias, M. Fraga, and J. A. Costoya, "Defining hypoxic microenvironments by non-invasive functional optical imaging," *Eur. J. Cancer*, vol. 49, no. 1, pp. 264–271, 2013, doi: 10.1016/j.ejca.2012.06.001.

[87] J. B. Wu *et al.*, "Near-infrared fluorescence imaging of cancer mediated by tumor hypoxia and HIF1α/OATPs signaling axis," *Biomaterials*, vol. 35, no. 28, pp. 8175–8185, 2014, doi: https://doi.org/10.1016/j.biomaterials.2014.05.073.

[88] M. López-Lázaro, "Dual role of hydrogen peroxide in cancer: Possible relevance to cancer chemoprevention and therapy," *Cancer Lett.*, vol. 252, no. 1, pp. 1–8, 2007, doi: 10.1016/j.canlet.2006.10.029.

[89] G. C. Van de Bittner, E. A. Dubikovskaya, C. R. Bertozzi, and C. J. Chang, "In vivo imaging of hydrogen peroxide production in a murine tumor model with a chemoselective bioluminescent reporter," *Proc. Natl. Acad. Sci.*, vol. 107, no. 50, pp. 21316–21321, 2010, doi: 10.1073/pnas.1012864107.

[90] N. A. Sieracki *et al.*, "Bioluminescent detection of peroxynitrite with a boronic acid-caged luciferin," *Free Radic. Biol. Med.*, vol. 61, pp. 40–50, 2013, doi: 10.1016/j.freeradbiomed.2013.02.020.

[91] J. Zielonka, R. Podsiadły, M. Zielonka, M. Hardy, and B. Kalyanaraman, "On the use of peroxy-caged luciferin (PCL-1) probe for bioluminescent detection of inflammatory oxidants in vitro and in vivo – Identification of reaction intermediates and oxidant-specific minor products," *Free Radic. Biol. Med.*, vol. 99, pp. 32–42, 2016, doi: 10.1016/j.freeradbiomed.2016.07.023.

[92] Y. C. Chae *et al.*, "Mitochondrial Akt Regulation of Hypoxic Tumor Reprogramming," *Cancer Cell*, vol. 30, no. 2, pp. 257–272, 2016, doi: 10.1016/j.ccell.2016.07.004.

[93] E. H. Moriyama *et al.*, "The influence of hypoxia on bioluminescence in luciferase-transfected gliosarcoma tumor cells in vitro," *Photochem.*

Photobiol. Sci., vol. 7, no. 6, pp. 675–680, 2008, doi: 10.1039/b719231b.

[94] T. Heishi *et al.*, "Endogenous Angiogenesis Inhibitor Vasohibin1 Exhibits Broad-Spectrum Antilymphangiogenic Activity and Suppresses Lymph Node Metastasis," *Am. J. Pathol.*, vol. 176, no. 4, pp. 1950–1958, 2010, doi: https://doi.org/10.2353/ajpath.2010.090829.

[95] S. K. Lyons *et al.*, "Non-invasive in vivo bioluminescent imaging of tumor angiogenesis in mice," *Cancer Res.*, vol. 65, no. 9, pp. 903–903, May 2005.

[96] W. Barry Edwards *et al.*, "Multimodal imaging of integrin receptor-positive tumors by bioluminescence, fluorescence, gamma scintigraphy, and single-photon emission computed tomography using a cyclic RGD peptide labeled with a near-infrared fluorescent dye and a radionuclide," *Mol. Imaging*, vol. 8, no. 2, pp. 101–110, 2009, doi: 10.2310/7290.2009.00014.

[97] H. Zhao *et al.*, "Apj+ Vessels Drive Tumor Growth and Represent a Tractable Therapeutic Target," *Cell Rep.*, vol. 25, no. 5, pp. 1241–1254, 2018, doi: 10.1016/j.celrep.2018.10.015.

[98] B. Mansoori, A. Mohammadi, S. Davudian, S. Shirjang, and B. Baradaran, "The different mechanisms of cancer drug resistance: A brief review," *Adv. Pharm. Bull.*, vol. 7, no. 3, pp. 339–348, 2017, doi: 10.15171/apb.2017.041.

[99] L. Yu *et al.*, "Estrogen-independent Myc overexpression confers endocrine therapy resistance on breast cancer cells expressing ERαY537S and ERαD538G mutations," *Cancer Lett.*, vol. 442, pp. 373–382, 2019, doi: https://doi.org/10.1016/j.canlet.2018.10.041.

[100] M. Vooijs, J. Jonkers, S. Lyons, and A. Berns, "Noninvasive imaging of spontaneous retinoblastoma pathway-dependent tumors in mice," *Cancer Res*, vol. 62, no. 6, pp. 1862–1867, 2002.

[101] B. Li *et al.*, "A Novel Bioluminescence Orthotopic Mouse Model for Advanced Lung Cancer," *Radiat. Res.*, vol. 176, no. 4, pp. 486–493, 2011.

[102] R. J. Viola *et al.*, "In Vivo Bioluminescence Imaging Monitoring of Hypoxia-Inducible Factor 1α, a Promoter That Protects Cells, in Response to Chemotherapy," *Am. J. Roentgenol.*, vol. 191, no. 6, pp. 1779–1784, Dec. 2008, doi: 10.2214/AJR.07.4060.

[103] J. A. Horton, J. A. Strauss, M. J. Allen, and T. A. Damron, "Physeal bystander effects in rhabdomyosarcoma radiotherapy: Experiments in a new xenograft model," *Sarcoma*, vol. 2011, no. 1, 2011, doi: 10.1155/2011/815190.

[104] B. Zhang *et al.*, "Bioluminescence Tomography-Guided Radiation Therapy for Preclinical Research.," *Int. J. Radiat. Oncol. Biol. Phys.*, vol. 94, no. 5, pp. 1144–53, Apr. 2016, doi: 10.1016/j.ijrobp.2015.11.039.

[105] American Cancer Society, "What Is Cancer Immunotherapy?," 2016. [Online]. Available: https://www.cancer.org/treatment/treatments-and-side-effects/treatment-types/immunotherapy.html.

[106] H. R. Mirzaei, H. Mirzaei, S. Yun Lee, J. Hadjati, and B. G. Till, "Prospects for chimeric antigen receptor (CAR) γδ T cells: A potential game changer for adoptive T cell cancer immunotherapy," *Cancer Letters*, vol. 380, no. 2. Elsevier Ireland Ltd, pp. 413–423, 2016, doi: 10.1016/j.canlet.2016.07.001.

[107] H. Rozemuller *et al.*, "A bioluminescence imaging based in vivo model for preclinical testing of novel cellular immunotherapy strategies to improve the graft-versus-myeloma effect.," *Haematologica*, vol. 93, no. 7, pp. 1049–1057, Jul. 2008, doi: 10.3324/haematol.12349.

[108] W. Maes and K. U. Leuven, "In vivo bioluminescence imaging in an experimental mouse model for dendritic cell based immunotherapy against malignant glioma," *Artic. J. Neuro-Oncology*, vol. 91, no. 2, pp. 127–139, 2009, doi: 10.1007/s11060-008-9691-5.

[109] S. L. Ginn, A. K. Amaya, I. E. Alexander, M. Edelstein, and M. R. Abedi, "Gene therapy clinical trials worldwide to 2017: An update," *J. Gene Med.*, vol. 20, no. 5, p. e3015, 2018, doi: 10.1002/jgm.3015.

[110] E. Mullin, "A pioneering gene therapy for leukemia has arrived in the U.S," *MIT Technology Review*, 2017. [Online]. Available: https://www.technologyreview.com/2017/08/30/149399/the-fda-has-approved-the-first-gene-therapy-for-cancer/. [Accessed: 05-Dec-2018].

[111] D. Cross and J. K. Burmester, "Gene therapy for cancer treatment: Past, present and future," *Clin. Med. Res.*, vol. 4, no. 3, pp. 218–227, 2006, doi: 10.3121/cmr.4.3.218.

[112] Z. Saadatpour *et al.*, "Molecular imaging and cancer gene therapy," *Cancer Gene Ther.*, Nov. 2016, doi: 10.1038/cgt.2016.62.

[113] Z. Saadatpour *et al.*, "Imaging techniques: New avenues in cancer gene and cell therapy," *Cancer Gene Therapy*, vol. 24, no. 1. Nature Publishing Group, pp. 1–5, 01-Jan-2017, doi: 10.1038/cgt.2016.61.

[114] Z. Zhang, L. Liu, S. Cao, Y. Zhu, and Q. Mei, "Gene delivery of TIPE2 inhibits breast cancer development and metastasis via CD8+T and NK cell-mediated antitumor responses," *Mol. Immunol.*, vol. 85, pp. 230–237, 2017, doi: 10.1016/j.molimm.2017.03.007.

[115] G. M. Proshkina, E. I. Shramova, O. N. Shilova, A. V Ryabova, and S. M. Deyev, "Phototoxicity of flavoprotein miniSOG induced by bioluminescence resonance energy transfer in genetically encoded system NanoLuc-miniSOG is comparable with its LED-excited phototoxicity," *J. Photochem. Photobiol. B Biol.*, vol. 188, pp. 107–115, 2018, doi: 10.1016/j.jphotobiol.2018.09.006.

[116] C. A. Maguire *et al.*, "Triple bioluminescence imaging for in vivo monitoring of cellular processes," *Mol. Ther. - Nucleic Acids*, vol. 2, no. 6, p. e99, 2013, doi: 10.1038/mtna.2013.25.

[117] T. Rhim, D. Y. Lee, and M. Lee, "Hypoxia as a target for tissue specific gene therapy," *J. Control. Release*, vol. 172, no. 2, pp. 484–494, 2013, doi: 10.1016/j.jconrel.2013.05.021.

[118] S. Bortolanza *et al.*, "Treatment of pancreatic cancer with an oncolytic adenovirus expressing interleukin-12 in Syrian hamsters," *Mol. Ther.*, vol. 17, no. 4, pp. 614–622, 2009, doi: 10.1038/mt.2009.9.

[119] Y. Zhang *et al.*, "Escherichia coli Nissle 1917 targets and restrains mouse b16 melanoma and 4T1 breast tumors through expression of azurin protein," *Appl. Environ. Microbiol.*, vol. 78, no. 21, pp. 7603–7610, 2012, doi: 10.1128/AEM.01390-12.

[120] L. H. Dang, C. Bettegowda, D. L. Huso, K. W. Kinzler, and B. Vogelstein, "Combination bacteriolytic therapy for the treatment of experimental tumors," *Proc. Natl. Acad. Sci.*, vol. 98, no. 26, pp. 15155–15160, 2001, doi: 10.1073/pnas.251543698.

[121] L. J. Jia *et al.*, "Enhanced therapeutic effect by combination of tumor-targeting salmonella and endostatin in murine melanoma model," *Cancer Biol. Ther.*, vol. 4, no. 8, pp. 840–845, Aug. 2005, doi: 10.4161/cbt.4.8.1891.

[122] R. Li *et al.*, "Expressing Cytotoxic Compounds in Escherichia coli Nissle 1917 for Tumor-targeting Therapy," *Res. Microbiol.*, vol. 170, no. 2, pp. 74–79, 2018, doi: 10.1016/J.RESMIC.2018.11.001.

[123] S. Indraccolo, S. Walenta, and W. Mueller-Klieser, "Uncovering metabolic effects of anti-angiogenic therapy in tumors by induced metabolic bioluminescence imaging," *Methods Mol. Biol.*, vol. 1464, no. February, pp. 175–184, 2016, doi: 10.1007/978-1-4939-3999-2_16.

[124] M. Keshavarzi *et al.*, "Molecular Imaging and Oral Cancer Diagnosis and Therapy," *J. Cell. Biochem.*, vol. 118, no. 10, pp. 3055–3060, 2017, doi: 10.1002/jcb.26042.

[125] T. V. Sekar, R. K. Mohanram, K. Foygel, and R. Paulmurugan, "Therapeutic evaluation of microRNAs by molecular imaging," *Theranostics*, vol. 3, no. 12, pp. 964–985, 2013, doi: 10.7150/thno.4928.

[126] R. Moradian Tehrani *et al.*, "Mesenchymal stem cells: A new platform for targeting suicide genes in cancer," *J. Cell. Physiol.*, vol. 233, no. 5, pp. 3831–3845, 2018, doi: 10.1002/jcp.26094.

[127] A. Tivnan, N. H. Foley, L. Tracey, A. M. Davidoff, and R. L. Stallings, "MicroRNA-184-mediated inhibition of tumour growth in an orthotopic murine model of neuroblastoma," *Anticancer Res.*, vol. 30, no. 11, pp. 4391–4395, 2010.

[128] Z. Zhou, X. Niu, C. Li, S. Sheng, and S. Lu, "Inhibition of the growth of non-small cell lung cancer by miRNA-1271," *Am. J. Transl. Res.*, vol. 7, no. 10, pp. 1917–1924, 2015.

[129] M. Perepelyuk, K. Sacko, K. Thangavel, and S. A. Shoyele, "Evaluation of MUC1-Aptamer Functionalized Hybrid Nanoparticles for Targeted Delivery of miRNA-29b to Nonsmall Cell Lung Cancer," *Mol. Pharm.*, vol. 15, no. 3, pp. 985–993, 2018, doi: 10.1021/acs.molpharmaceut.7b00900.

[130] F. Wang *et al.*, "Imaging Dendrimer-Grafted Graphene Oxide Mediated Anti-miR-21 Delivery with an Activatable Luciferase Reporter," *ACS Appl. Mater. Interfaces*, vol. 8, no. 14, pp. 9014–9021, 2016, doi: 10.1021/acsami.6b02662.

[131] F. Takeshita, R. U. Takahashi, J. Onodera, and T. Ochiya, "In vivo imaging of oligonucleotide delivery," *Methods Mol. Biol.*, vol. 52, pp. iv40–iv47, 2012, doi: 10.1007/978-1-61779-797-2_17.

[132] A. Iscaife *et al.*, "Treating metastatic prostate cancer with microRNA-145," *Apoptosis*, vol. 23, no. 7–8, pp. 388–395, 2018, doi: 10.1007/s10495-018-1461-z.

[133] Y. L. Chang, Y. C. Chou, and S. H. Chiou, "Curcumin attenuates tumor initiating stem-like property of head and neck cancer through miR145/SOX9/ADAM17 axis," *Clin. Pharmacol. Ther.*, vol. 73, no. 8, 2013.

[134] M. Hikichi and T. Nakamura, "Systemic Cancer Virotherapy with

MDVV, a Combined miRNA-Regulated and Thymidine Kinase-Deleted Oncolytic Vaccinia Virus," *Mol. Ther.*, vol. 20, no. 1, p. S79, 2012, doi: 10.1016/s1525-0016(16)36005-1.

[135] J. Wang and J. V Jokerst, "Stem Cell Imaging: Tools to Improve Cell Delivery and Viability," *Stem Cells Int.*, vol. 2016, 2016, doi: 10.1155/2016/9240652.

[136] H. Mirzaei *et al.*, "Therapeutic application of multipotent stem cells," *J. Cell. Physiol.*, vol. 233, no. 4, pp. 2815–2823, 2018, doi: 10.1002/jcp.25990.

[137] R. Moradian Tehrani *et al.*, "Mesenchymal stem cells: A new platform for targeting suicide genes in cancer," *J. Cell. Physiol.*, vol. 233, no. 5, pp. 3831–3845, May 2018, doi: 10.1002/jcp.26094.

[138] T. Yang *et al.*, "Enhancing the therapeutic effect via elimination of hepatocellular carcinoma stem cells using Bmi1 siRNA delivered by cationic cisplatin nanocapsules," *Nanomedicine Nanotechnology, Biol. Med.*, vol. 14, no. 7, pp. 2009–2021, 2018, doi: https://doi.org/10.1016/j.nano.2018.05.012.

[139] Y. Xiao *et al.*, "Integrin α5 down-regulation by miR-205 suppresses triple negative breast cancer stemness and metastasis by inhibiting the Src/Vav2/Rac1 pathway," *Cancer Lett.*, vol. 433, pp. 199–209, 2018, doi: https://doi.org/10.1016/j.canlet.2018.06.037.

[140] B. Humphries *et al.*, "MicroRNA-200b targets protein kinase Cα and suppresses triple-negative breast cancer metastasis," *Carcinogenesis*, vol. 35, no. 10, pp. 2254–2263, Oct. 2014.

[141] "pMirTarget 3'-UTR Assay Vector," *origene.com*. [Online]. Available: https://www.origene.com/catalog/vectors/3-utr-assay-vector/ps100062/pmirtarget-3-utr-assay-vector. [Accessed: 07-Dec-2018].

[142] A. Al Faraj, A. S. Shaik, E. Ratemi, and R. Halwani, "Combination of drug-conjugated SWCNT nanocarriers for efficient therapy of cancer stem cells in a breast cancer animal model," *J. Control. Release*, vol. 225, pp. 240–251, 2016, doi: https://doi.org/10.1016/j.jconrel.2016.01.053.

[143] J. H. Chen, A. T.H Wu, D. T.W Tzeng, C. C. Huang, Y. M. Tzeng, and T. Y. Chao, "Antrocin, a bioactive component from Antrodia cinnamomea, suppresses breast carcinogenesis and stemness via downregulation of β-catenin/Notch1/Akt signaling," *Phytomedicine*, vol. 52, pp. 70–78, 2019, doi: https://doi.org/10.1016/j.phymed.2018.09.213.

[144] L. Leng *et al.*, "Molecular imaging for assessment of mesenchymal stem cells mediated breast cancer therapy," *Biomaterials*, vol. 35, no. 19, pp. 5162–5170, 2014, doi: https://doi.org/10.1016/j.biomaterials.2014.03.014.

[145] H. J. Paholak *et al.*, "Elimination of epithelial-like and mesenchymal-like breast cancer stem cells to inhibit metastasis following nanoparticle-mediated photothermal therapy," *Biomaterials*, vol. 104, pp. 145–157, 2016, doi: https://doi.org/10.1016/j.biomaterials.2016.06.045.

[146] S. A. Choi *et al.*, "Histone deacetylase inhibitor panobinostat potentiates the anti-cancer effects of mesenchymal stem cell-based sTRAIL gene therapy against malignant glioma," *Cancer Lett.*, vol. 442, pp. 161–169, 2019, doi: https://doi.org/10.1016/j.canlet.2018.10.012.

[147] J. Dong *et al.*, "Bisacodyl and its cytotoxic activity on human glioblastoma stem-like cells. Implication of inositol 1,4,5-triphosphate receptor dependent calcium signaling," *Biochim. Biophys. Acta - Mol. Cell Res.*, vol. 1864, no. 6, pp. 1018–1027, 2017, doi: https://doi.org/10.1016/j.bbamcr.2017.01.010.

[148] B. Liu *et al.*, "lncRNA GAS5 Reverses EMT and Tumor Stem Cell-Mediated Gemcitabine Resistance and Metastasis by Targeting miR-221/SOCS3 in Pancreatic Cancer," *Mol. Ther. - Nucleic Acids*, vol. 13, pp. 472–482, 2018, doi: https://doi.org/10.1016/j.omtn.2018.09.026.

[149] P. T. Yin, S. Shah, N. J. Pasquale, O. B. Garbuzenko, T. Minko, and K. B. Lee, "Stem cell-based gene therapy activated using magnetic hyperthermia to enhance the treatment of cancer," *Biomaterials*, vol. 81, pp. 46–57, 2016, doi: 10.1016/j.biomaterials.2015.11.023.

[150] T. Mašek, V. Vopalenský, and M. Pospíšek, "The Luc2 gene enhances reliability of bicistronic assays," *Cent. Eur. J. Biol.*, vol. 8, no. 5, pp. 423–431, 2013, doi: 10.2478/s11535-013-0151-z.

[151] B. Humphries, Z. Wang, Y. Li, J. R. Jhan, Y. Jiang, and C. Yang, "ARHGAP18 Downregulation by miR-200b Suppresses Metastasis of Triple-Negative Breast Cancer by Enhancing Activation of RhoA," *Cancer Res.*, vol. 77, no. 15, pp. 4051–4064, Jun. 2017, doi: 10.1158/0008-5472.CAN-16-3141.

[152] L. Zhang, M. S. Bhojani, B. D. Ross, and A. Rehemtulla, "Enhancing akt imaging through targeted reporter expression," *Mol. Imaging*, vol. 7, no. 4, pp. 168–174, 2008, doi: 10.2310/7290.2008.00017.

[153] M. P. Lisanti *et al.*, "Hydrogen peroxide fuels aging, inflammation, cancer metabolism and metastasis: The seed and soil also needs 'fertilizer,'" *Cell Cycle*, vol. 10, no. 15, pp. 2440–2449, 2011, doi: 10.4161/cc.10.15.16870.

[154] C. Gregor, K. C. Gwosch, S. J. Sahl, and S. W. Hell, "Strongly enhanced bacterial bioluminescence with the ilux operon for single-cell imaging," *Proc. Natl. Acad. Sci.*, vol. 115, no. 5, pp. 962–967, 2018, doi: 10.1073/pnas.1715946115.

[155] M. L. Foucault, L. Thomas, S. Goussard, B. R. Branchini, and C. Grillot-Courvalin, "In vivo bioluminescence imaging for the study of intestinal colonization by Escherichia coli in mice," *Appl. Environ. Microbiol.*, vol. 76, no. 1, pp. 264–274, 2010, doi: 10.1128/AEM.01686-09.

[156] N. Andreu *et al.*, "Optimisation of bioluminescent reporters for use with mycobacteria," *PLoS One*, vol. 5, no. 5, p. e10777, 2010, doi: 10.1371/journal.pone.0010777.

[157] B. A. Tannous, D. E. Kim, J. L. Fernandez, R. Weissleder, and X. O. Breakefield, "Codon-optimized gaussia luciferase cDNA for mammalian gene expression in culture and in vivo," *Mol. Ther.*, vol. 11, no. 3, pp. 435–443, 2005, doi: 10.1016/j.ymthe.2004.10.016.

[158] T. Wurdinger *et al.*, "A secreted luciferase for ex vivo monitoring of in vivo processes," *Nat. Methods*, vol. 5, no. 2, pp. 171–173, 2008, doi: 10.1038/nmeth.1177.

[159] M. T. Alonso, M. Rodríguez-Prados, P. Navas-Navarro, J. Rojo-Ruiz, and J. García-Sancho, "Using aequorin probes to measure Ca2+ in intracellular organelles," *Cell Calcium*, vol. 64, pp. 3–11, 2017, doi: https://doi.org/10.1016/j.ceca.2017.01.006.

[160] M. P. Hall *et al.*, "Engineered luciferase reporter from a deep sea shrimp utilizing a novel imidazopyrazinone substrate," *ACS Chem. Biol.*, vol. 7, no. 11, pp. 1848–1857, 2012, doi: 10.1021/cb3002478.

[161] T. L. Riss, "NanoLuc: A Smaller, Brighter, More Versatile Luciferase Reporter." [Online]. Available: https://www.promega.com/%7B~%7D/media/files/promega. [Accessed: 06-Dec-2018].

[162] K. Suzuki *et al.*, "Five colour variants of bright luminescent protein for real-time multicolour bioimaging," *Nat. Commun.*, vol. 7, p. 13718, 2016, doi: 10.1038/ncomms13718.

[163] E. A. Meighen, "Molecular biology of bacterial bioluminescence.," *Microbiol. Rev.*, vol. 55, no. 1, pp. 123–142, Mar. 1991.

[164] W. Paschen, "Regional Quantitative Determination of Lactate in Brain Sections. A Bioluminescent Approach," *J. Cereb. Blood Flow Metab.*, vol. 5, no. 4, pp. 609–612, Dec. 1985, doi: 10.1038/jcbfm.1985.90.

[165] P. Tamulevicius and C. Streffer, "Metabolic imaging in tumours by means of bioluminescence.," *Br. J. Cancer*, vol. 72, no. 5, pp. 1102–12, Nov. 1995.

[166] W. Mueller-klieser, S. Walenta, W. Paschen, F. Kallinowski, and P. Vaupel, "Metabolic imaging in microregions of tumors and normal tissues with bioluminescence and photon counting," *J. Natl. Cancer Inst.*, vol. 80, no. 11, pp. 842–848, 1988, doi: 10.1093/jnci/80.11.842.

[167] C. Wang *et al.*, "Optical molecular imaging for tumor detection and image-guided surgery," *Biomaterials*, vol. 157, pp. 62–75, Mar. 2018, doi: 10.1016/J.BIOMATERIALS.2017.12.002.

[168] Y. Wang, M. Iyer, A. Annala, L. Wu, M. Carey, and S. S. Gambhir, "Noninvasive indirect imaging of vascular endothelial growth factor gene expression using bioluminescence imaging in living transgenic mice," *Physiol. Genomics*, vol. 24, no. 2, pp. 173–180, Feb. 2006, doi: 10.1152/physiolgenomics.00308.2004.

[169] H. Fan-Minogue *et al.*, "Noninvasive molecular imaging of c-Myc activation in living mice.," *Proc. Natl. Acad. Sci. U. S. A.*, vol. 107, no. 36, pp. 15892–15897, Sep. 2010, doi: 10.1073/pnas.1007443107.

[170] A. Godinat *et al.*, "A Biocompatible in Vivo Ligation Reaction and Its Application for Noninvasive Bioluminescent Imaging of Protease Activity in Living Mice," *ACS Chem. Biol.*, vol. 8, no. 5, pp. 987–999, May 2013, doi: 10.1021/cb3007314.

[171] A. Rehemtulla *et al.*, "Rapid and quantitative assessment of cancer treatment response using in vivo bioluminescence imaging," *Neoplasia*, vol. 2, no. 6, pp. 491–495, Jan. 2000, doi: 10.1038/sj.neo.7900121.

[172] S. K. Lyons, R. Meuwissen, P. Krimpenfort, and A. Berns, "The generation of a conditional reporter that enables bioluminescence imaging of Cre/loxP-dependent tumorigenesis in mice.," *Cancer Res.*, vol. 63, no. 21, pp. 7042–6, Nov. 2003.

[173] L. Gu, W. M. Tsark, D. A. Brown, S. Blanchard, T. W. Synold, and S. E. Kane, "A new model for studying tissue-specific mdr1a gene expression in vivo by live imaging.," *Proc. Natl. Acad. Sci. U. S. A.*, vol.

106, no. 13, pp. 5394–5399, Mar. 2009, doi: 10.1073/pnas.0807343106.
[174] E. Angst, M. Chen, M. Mojadidi, O. J. Hines, H. A. Reber, and G. Eibl, "Bioluminescence Imaging of Angiogenesis in a Murine Orthotopic Pancreatic Cancer Model," *Mol. Imaging Biol.*, vol. 12, no. 6, pp. 570–575, 2010, doi: 10.1007/s11307-010-0310-4.
[175] R. Zhong, M. Pytynia, C. Pelizzari, and M. Spiotto, "Bioluminescent Imaging of HPV-Positive Oral Tumor Growth and Its Response to Image-Guided Radiotherapy," *Cancer Res.*, vol. 74, no. 7, pp. 2073–2081, Apr. 2014, doi: 10.1158/0008-5472.CAN-13-2993.
[176] J. Shi, T. S. Udayakumar, Z. Wang, N. Dogan, A. Pollack, and Y. Yang, "Optical molecular imaging-guided radiation therapy part 1: Integrated x-ray and bioluminescence tomography," *Med. Phys.*, vol. 44, no. 9, pp. 4786–4794, Sep. 2017, doi: 10.1002/mp.12415.

TABLE III
CHRONOLOGICAL SUMMARY OF *IN VITRO* STUDIES PERTAINING TO CANCER APPLICATIONS OF BIOLUMINESCENCE IMAGING (BLI)

Author (year)	Application	Cancer Type	Main Findings
Wang et al. [168] (2006)	Imaging angiogenesis	Human cervical cancer and mouse mammary tumor (NK2)	1. Bioluminescence activity three-fold greater in the two-step transcriptional amplification system. 2. Detection of bioluminescence signal within 4 days of inoculation. 3. Peak bioluminescence signals obtained on the 14th day.
Coppola et al. [70] (2008)	Imaging apoptosis	D54 glioblastoma cells	1. Treatment with temozolomide and perifosine induced bioluminescence activity and activation of caspase-3. 2. Treatment with temozolomide and radiation increased bioluminescence activity and enhanced apoptosis.
Maes et al. [108] (2009)	Imaging response to immunotherapy	Murine glioma cells (GL261)	1. Measured BLI signal adequate measurement of luciferase activity in mouse brain glioma model. 2. *In vivo* BLI signal correlated with *ex vivo* BLI values and *in vitro* luminometric measurements.
Bortolanza et al. [118] (2009)	Imaging for gene therapy	Pancreatic cancer	1. Bioluminescence signal used to measure impact of E1A CR2 deletion. 2. Bioluminescence used to image response of modified viral genes (CRAds) to HIF-1.
Fan-Minogue et al. [169] (2010)	Imaging Tumorigenesis and metastasis	SKBR3 cells (breast cancer cells)	1. Developed sensor enables imaging of S62 phosphorylation. 2. Sensor signal correlated with endogenous c-Myc phosphorylation level in cells and living mice.
Scabini et al. [71] (2011)	Imaging apoptosis	human colon cancer cell line (HCT116) and the human glioblastoma cell line (U251)	1. Mice treated with camptothecin and temozolomide showed 2-fold induction of Z-DEVD-aminoluciferin luminescent signal compared to untreated group.
Godinat et al. [170] (2013)	Imaging apoptosis	Ovarian and breast cancer cells	1. Greater signal obtained from animals treated with lipopolysaccharide and D-galactosamine. 2. 2-fold increase in signal observed in mice treated with docetaxel.
Wu et al. [87] (2014)	Imaging tumor hypoxia	Human prostate cancer cells (PC-3)	1. Increase in bioluminescence signal due to HRE expression and HIF-1 activity, which correlate to tumor hypoxia. 2. Time-dependent increase in bioluminescence signal with increased HIF-1 expression.
Suchowski et al. [69] (2017)	Imaging tumor hypoxia and response to chemotherapy	Non-small cell lung cancer	1. 8 to 13-fold increase in reporter activity after erlotinib administration proving BLI could be used for AKT inhibitive chemotherapy.
Morciano et al. [67] (2017)	Imaging cancer metabolism	Malignant melanoma (MZ2-MEL) and human ovarian carcinoma cells (OVCAR-3)	1. Optimized protocols for monitoring ATP concentrations in cytosol, mitochondrial matrix and peri-cellular space. 2. A detailed protocol for detection of extracellular ATP in mice using luciferase-transfected reporter cells was developed.
Zhang et al. [114] (2017)	Imaging response to gene therapy	Metastatic breast cancer (4T1)	1. Luciferase expression was used to image metastatic tumor nodules. 2. Decreased tumor sizes were found in TIPE2 group using BLI.
Proshkina et al. [115] (2018)	Imaging response to gene therapy	Human breast adenocarcinoma cells (SK-BR-3)	1. Light emission using NanoLuc found to be comparable with LED-dosage.
Li et al. [122] (2018)	Imaging response to gene therapy	Human osteosarcoma (U-2); human head and neck squamous cell carcinoma (UT-SCC-5)	1. Bioluminescent E.coli used to ensure tumor-specific colonization. 2. Bioluminescent E.coli for expression of cytotoxic drugs able to repress tumor growth.
Yang et al. [138] (2018)	Imaging response to stem cell therapy	Liver hepatocellular carcinoma (HEPG2 cells)	1. 5 tumor nodules found in the NPC/Bmi1siR group compared to 18 and 22 nodules found in the NPC and cisplatin control groups. 2. BLI used to visualize NPCs reaching tumor site and clearing after 12 hours.
Liu et al. [59] (2018)	Imaging metastasis and response to gene therapy	Human breast cancer (MDA-MB-231, MCF7, BT549, MDA-MB-453, MDA-MB-468 and T47D)	1. Luciferase activity measured in conjunction with real-time PCR to quantitate EMT-related miRNA activity, miR-200c. 2. Lower levels of miRNA-200c expression associated with lower metastasis and therefore, can be used to measure efficacy of treatments.

TABLE IV
CHRONOLOGICAL SUMMARY OF *IN VIVO* STUDIES PERTAINING TO CANCER APPLICATIONS OF BIOLUMINESCENCE IMAGING (BLI)

Author (year)	Application	Animal Model	Cancer Type	Main Findings
Kozlowski et al. [52] (1984)	Imaging tumorigenesis and metastasis	Athymic BALB/c nude mice	Malignant melanoma; colon carcinoma; prostate adenoma; renal adenocarcinoma	1. Light emissions detectable within minutes of injecting tumor cells. 2. Signals continued to increase logarithmically over a 2 week period.
Streffer and Tamulevicius [165] (1995)	Imaging cancer metabolism	NMRI nude mice	Squamous head and neck carcinoma	1. High concentrations of ATP and glucose in viable cell regions. 2. High lactate levels in necrotic tumor centers. 3. Lactate diffusely distributed over sections with highly localized ATP. 3. Good agreement between mean values of cryo-sections using bioluminescence with sections obtained by conventional methods.
Sweeney et al. [51], [53] (1999)	Imaging tumorigenesis and metastasis	Severe combined immunodeficiency mice	HeLa cells (human cervical cancer cells)	1. Untreated animals showed progressive increases in signal intensity over time. 2. Animals treated with cisplatin had marked reductions in tumor signal. 3. 5-fluorouracil was less effective while cyclophosphamide was ineffective. 4. Immunotherapy reduced signals at high effector-to-target cell ratios.
Rehemtulla et al. [171] (2000)	Imaging tumorigenesis and metastasis	Nude mice	9L gliosarcoma cells (rat brain tumor cells)	1. Excellent correlation between detected photons and tumor volume. 2. Similar cell kill values obtained from MRI volume measurements and BLI photon counts.
Lyons et al. [172] (2003)	Imaging tumorigenesis and metastasis	Cre/loxP-dependent mice	Lung cancer	1. Bioluminescence "switched-on" in Cre-dependent manner. 2. 4 and 6-log increase in light emission per mg of wet tissue weight.
Pellegatti et al. [68] (2008)	Imaging cancer metabolism	Nude mice	Human embryonic kidney cells (HEK293) and human ovarian carcinoma cells (OVCAR-3)	1. *In vivo* detection of high extracellular ATP concentration at tumor sites.
Viola et al. [102] (2008)	Imaging response to chemotherapy	BALB/c mice	4T1 murine breast carcinoma cells	1. Cyclophosphamide inhibited tumor growth and increased HIF-1 protein levels.
Rozemuller et al. [107] (2008)	Imaging response to immunotherapy	RAG2-mice.	Multiple myeloma cell lines	1. Tumors treated with radiotherapy showed temporary regression. 2. Infusion of allogeneic peripheral blood mononuclear cells resulted in complete eradication of tumors.
Maes et al. [108] (2009)	Imaging response to immunotherapy	C57BL/6 J-Tyrc^{-2} $^{J/J}$ mice	Murine glioma cells (GL261)	1. Measured BLI signal adequate measurement of luciferase activity in mouse brain glioma model. 2. *In vivo* BLI signal correlated with *ex vivo* BLI values and *in vitro* luminometric measurements.
Gu et al. [173] (2009)	Imaging response to immunotherapy	Nude mice	-	1. *mdr*1a,*fLUC* insertion yielded luminescence intensities parallel to endogenous *mdr*1a mRNA expression.
Edwards et al. [96] (2009)	Imaging angiogenesis	NCR nude mice	Mouse breast tumor (4T1- Luc cells)	1.4T1 cells transfected with FLuc reporter gene increased uptake of synthesized probe targeting $\alpha_v\beta_3$ integrin. 2. Areas of high $\alpha_v\beta_3$ expression within tumor clearly identified using BLI and SPECT.
Fan-Minogue et al. [169] (2010)	Imaging Tumorigenesis and metastasis	Nude mice	SKBR3 cells (breast cancer cells)	1. Developed sensor enables imaging of S62 phosphorylation. 2. Sensor signal correlated with endogenous c-Myc phosphorylation level in cells and living mice.
Angst et al. [174] (2010)	Imaging angiogenesis	VEGFR2-luc-K1 nude mice	Human pancreatic adenocarcinoma (HPAF-II pancreatic cancer cells)	1. 2.7-fold increase in light emission at tumor site. 2. Elevation in VEGFR2 promoter activity (angiogenesis).
Bhang et al. [54] (2011)	Imaging Tumorigenesis and metastasis	Nude mice	Human malignant melanoma; human breast cancer (MDA-MB-231)	1. Elevated gene-3 promoter used for detection of metastasis in murine human melanoma and breast cancer models. 2. Determination of sensitivity and specificity of system *in vivo* using radionuclide-based techniques.
Puaux et al. [56] (2011)	Imaging tumorigenesis and metastasis	Nude mice	B16 murine melanoma cells	1. BLI and FLI were the most practical techniques tested. 2. Both BLI and FDG-PET identified small nonpalpable tumors. 3. MRI and FLI only detected macroscopic, clinically evident tumors. 4. FDG-PET and MRI performed well in the identification of tumors.
Scabini et al. [71] (2011)	Imaging apoptosis	Male athymic nude mice	human colon cancer cell line (HCT116) and the human glioblastoma cell line (U251)	1. Mice treated with camptothecin and temozolomide showed 2-fold induction of Z-DEVD-aminoluciferin luminescent signal compared to untreated group.
Li et al. [101] (2011)	Imaging response to chemotherapy	Athymic nude mice	Human lung adenocarcinoma cells (A549)	1. Tumor responded to Paclitaxel and radiation indicated decreased tumor bioluminescence and improved overall survival.
Horton et al. [103] (2011)	Imaging response to radiotherapy	Skeletally immature mice	Rhabdomyosarcoma cells	1. 10Gray radiation reduced tumor growth velocity and prolonged but resulted in 3.3% shortening of irradiated limb. 2. 2Gray radiation dose resulted in 4.1% decrease in limb length but did not extend survival.
Goldman et al. [84] (2011)	Imaging tumor hypoxia	*MMTV-neu/beclin1+/-* mice	Murine mammary tumors	1. ODD-luciferase in transgenic mice emitted bioluminescence signal in regions of hypoxia. 2. Bioluminescence signal related to tumor size.
Zhong et al. [175] (2014)	Imaging response to radiotherapy	Triple transgenic mice containing the iHPV-Luc, K14-CreERtam and LSL-Kras transgenes	Oral tumors	1. Tamoxifen treatment resulted in 74.8-fold higher bioluminescence compared to control mice. 2. After treatment with rapamycin tumors regressed and possessed less bioluminescence.
Stollfuss et al. [55] (2015)	Imaging tumorigenesis and metastasis	Female nude mice	Gastric cancer cells	1. PET was more sensitive than BLI in detection of early peritoneal carcinomatosis in mouse model. 2. Sensitivity of BLI depended on the site of the lesions.
Indraccolo and Mueller-Klieser [66] (2016)	Imaging cancer metabolism	Severe combined immunodeficiency mice	Ovarian cancer cells (IGROV-1)	1. Quantification of lactate and glucose levels in tumor xenografts by imBLI was performed. 2. Bevacizumab-treated tumors contain large central necrosis. 3. High glucose concentrations are clearly seen in the tumor periphery.
Zhang et al. [104] (2016)	Imaging response to radiotherapy	Nude mice	-	1. Optical system capable of locating a target's center of mass with an accuracy of 1 mm. 2. Integrated BLT/CBCT system provided a solution for small, non-palpable, or orthotopic tumor models.
Suchowski et al. [69] (2017)	Imaging tumor hypoxia and response to chemotherapy	SCID beige mice	Non-small cell lung cancer	1. 8 to 13-fold increase in reporter activity after erlotinib administration proving BLI could be used for AKT inhibitive chemotherapy.
Shi et al. [176] (2017)	Imaging response of radiotherapy	-	Prostate tumor	1. BLT able to locate the bioluminescent tumors with < 0.5 mm error. 2. Tumor volume in BLT correlated with that in iodinated contrast CT. 2. Phantom experiments validated use of BLT in guided radiation therapy.
Zhao et al. [97] (2018)	Imaging tumor hypoxia and angiogenesis	-	Murine Lewis lung carcinoma (LLC), murine hepatocellular carcinoma cell line (Hepa1-6), human tetracarcinoma (TC-1)	1. Hypoxia successfully imaged using Apj-CreER and Apj-DTRGFP-Luciferase. 2. BLI used to prove that signal detection only for upregulated Apj$^+$ vessel cells.
Perepelyuk et al. [129] (2018)	Imaging response to gene therapy	-	Human alveolar basal epithelial cell line (A549)	1. miRNA-29 bloated hybrid nanoparticles (MAFMILHNs were shown to downregulate oncoprotein DNMT3B. 2. Tumor inhibition achieved due to downregulation of DNMT3B.